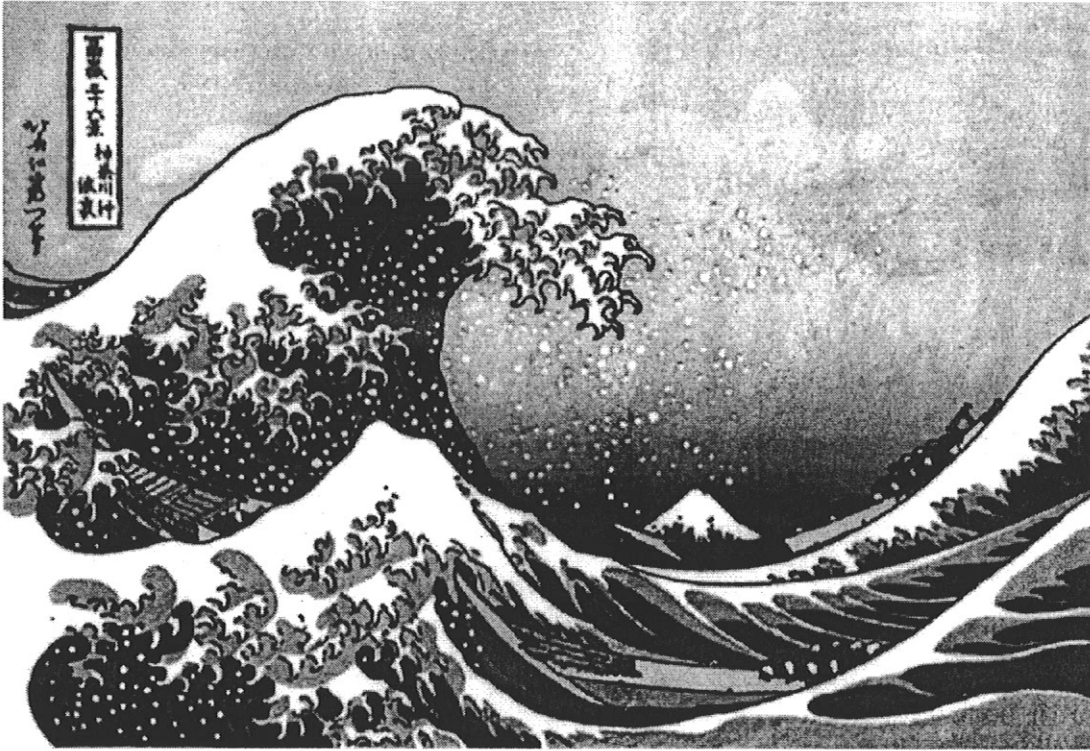


# Wave height prediction for island regions



**Research conducted at:**

University of Hawaii at Manoa  
Department of Ocean Engineering  
2540 Dole Street, Holmes Hall 402  
Honolulu, HI 96822  
U.S.A.

**By:**

Pascal Ferier  
Schoolstraat 10  
6411 CK Heerlen  
The Netherlands

**December 1996**

# Table of Contents

Abstract. . . . .	iii
List of figures . . . . .	v
List of tables. . . . .	vii
1. Introduction. . . . .	1
2. Refraction-diffraction nonlinear waves. . . . .	3
2.1. Project description. . . . .	3
2.1.1. Rationale. . . . .	3
2.1.2. Background. . . . .	3
2.1.3. Problem identification. . . . .	4
2.1.4. Goals and objectives. . . . .	4
2.1.5. Research methods/approach. . . . .	5
2.2. Green-Naghdi equations. . . . .	6
2.3. Analysis. . . . .	8
2.4. Results. . . . .	9
2.4.1. Set up # 1. . . . .	9
2.4.2. Set up # 2. . . . .	12
2.5. Discussion. . . . .	13

3.	Linear wave model verification.	.	.	.	.	.	.	14
3.1.	Project description.	.	.	.	.	.	.	14
3.1.1.	Rationale.	.	.	.	.	.	.	14
3.1.2.	Goals and objectives.	.	.	.	.	.	.	15
3.1.3.	Research methods/approach.	.	.	.	.	.	.	17
3.2.	Wave height predictions.	.	.	.	.	.	.	19
4.	References.	.	.	.	.	.	.	21
5.	Figures.	.	.	.	.	.	.	24

## Abstract

During the period from January 1996 until December 1996, I worked on two different projects at the Department of Ocean Engineering at the University of Hawaii at Manoa. The State Department of Civil Defense initiated these projects as a result of the 1992 hurricane Iniki, which devastated the Island of Kauai and damaged the other Hawaiian Islands as well. The objective of these projects is to develop a wave measurement database and field verified wave models for use by the public and private sectors.

The first project, which took up about 90 % of my time, deals with the development of computational capabilities to predict the refraction and diffraction of nonlinear, directional random waves in the nearshore environment. The Green-Naghdi (G-N) equations are used to determine the nonlinear diffraction of regular waves by topography in a numerical wave tank. In the first case, the Level II G-N equations are used to simulate monochromatic waves propagating over a steep shelf (slope 1:2) that reaches a height of 70 % of the fluid depth. These results are compared with experimental data of Ohyama et al. (1995) and the Level I G-N simulations of Ertekin and Becker (1996). In the second case, the accuracy of the Level II G-N equations is assessed for the nonlinear diffraction of monochromatic waves over a gentle shelf (slope 1:20) by comparing the numerical simulations with the measurements of Ohyama et al. (1994).

The results show that nonlinear diffraction is simulated more accurately over a larger range of wave frequencies by the Level II G-N equations than the Level I equations. The frequency range over which the Level II G-N equations accurately simulate wave propagation over both types of topography is consistent with the frequency range over which the Level II G-N equations accurately model linear dispersion (Shields and Webster, 1988). In addition, it is the frequency of the highest harmonic generated by the nonlinear interactions that limits the accuracy of the Level II G-N simulations. The present work also shows that the G-N equations can be used in accurately determining the nonlinear diffraction of waves by submerged bodies, such as oil storage tanks and

breakwaters. Thus the G-N equations may be used as an alternative to the solution of the fully nonlinear 3-D problem in modeling nonlinear diffraction.

The second project deals with the development of a methodology for estimating wave conditions at unmonitored coastal sites around the Hawaiian Islands specifically, but for reef-fringed islands in general.

Coastal field data is collected to test the accuracy of various wave transformation models. Model results are evaluated in the vicinity of reefs and at sites influenced by island sheltering. Computer simulations are used to determine the wave heights at selected sites at the South and West side of the Island of Oahu. At locations where the wave height increases considerably (hot spot), wave gages are deployed to measure the wave heights. These measurements will be compared with the computer simulations in order to verify the used computer models. A couple of the computer simulations have already been made and the wave gages are deployed as well. The comparison between the experimental data and the computer simulations is scheduled for the spring of 1997.

## List of figures

Figure 1 The Hawaiian Islands (degrees North and degrees West).	25
Figure 2 A schematic of the numerical wave tank used in Ertekin and Becker, 1996.	26
Figure 3 Comparison of the G-N results with the experiments of Ohyama et al. (1995) at wave gage G3 and G5. The free surface elevation, $\eta/H$ as a function of time $t/T$ for the following cases: (a) 2 at G3, (b) 2 at G5, (c) 4 at G3, (d) 4 at G5, (e) 6 at G3 and (f) 6 at G5. The circles refer to the experimental data of Ohyama et al. (1995), the solid line is the G-N II result and the dot-dash line is the G-N I result.	27
Figure 4 Spectral analysis of the experimental data (a, c, e) and the computer simulations (b, d, f) at wave gage 5 for case 2 (a) and (b), case 4 (c) and (d) and case 6 (e) and (f)	28
Figure 5a A schematic of the wave flume and the submerged bar used in the experiments of Ohyama et al (1994). All distances in meters.	29
Figure 5b A schematic of the numerical wave tank, modeling figure 3a. All distances in meters.	30
Figure 6 Comparison of the G-N II results with the experiments of Ohyama et al. (1994) at all gages for the long wave case. The free surface elevation, $\eta/H$ as a function of time $f_0 t$ . The circles refer to the experimental data of Ohyama et al. (1994) and the solid line is the G-N II result.	31
Figure 7 Comparison of the G-N II results with the experiments of Ohyama et al. (1994) at different gages for the short wave case. The free surface elevation, $\eta/H$ as a function of time $f_0 t$ at the following gages: (a) station 1, (b) station 3, (c) station 5 and (d) station 7. The circles refer to the experimental data of Ohyama et al. (1994) and the solid line is the G-N II result.	32
Figure 8 Locations of existing and proposed wave measurements in the Hawaiian region.	33
Figure 9 Primary sources of wave energy for the Hawaiian Islands, from Fletcher and Hwang, 1994.	34
Figure 10 Significant wave height and period at Makapu'u Point during Hurricane Iniki, from Fletcher and Hwang, 1994.	35

Figure 11 Wave height (m) for a single wave component for Waikiki beach.	36
Figure 12 Wave height (m) for a single wave component for Kailua Bay.	37
Figure 13 Two locations used for wave height simulation on the Island of Oahu.	38
Figure 14 Bathymetry (m) for Waikiki beach.	39
Figure 15 Bathymetry (m) for Kailua Bay.	40
Figure 16 Wave height (m) for Waikiki beach.	41
Figure 17 Wave height (m) for Kailua Bay.	42

## List of tables

Table 1	Wave parameters used in the calculations for set-up #1.	.	.	10
Table 2	Wave parameters used in the calculations for set-up #2.	.	.	12



## 1. Introduction

Although Hawaii seems to be paradise for most people, the islands of Hawaii (Fig. 1) face many natural threats. The most destructive of these natural disasters are the hurricanes and the tsunami's (long period wave generated by earthquakes). After hurricane Iniki hit the island of Kauai in 1992, the State Department of Civil Defense wanted to develop a wave measurement database and field verified wave models, which can be used by the public and private sectors. Based on this database, people at Civil Defense can take precautions whenever they think it is necessary.

The Department of Ocean Engineering at the University of Hawaii at Manoa was funded to conduct the measurements and develop the wave height prediction model. This project has started in August 1995 and is expected to be completed in July 1997. I have been a member of the project team from January 1996 until December 1996.

Most of my research was related to the development of computational capabilities to predict the refraction and diffraction of nonlinear, directional, random waves in the nearshore environment based on the input wave conditions offshore. It is necessary to develop a theoretical-numerical model for predictions, because it is not economically feasible to take measurements at a large number of sites.

The higher-order Green-Naghdi equations are used to model the wave transformation process that includes the effects of nonlinearity and steep bottom topography. A finite difference method is used to simulate the unsteady process. Actual bathymetry charts in digitized form will be used for variable water depth. The computer simulations will then be compared with direct ocean measurements.

The Green-Naghdi equations, the program used to do the numerical simulations, the simulations and the results are described in chapter 2.

Part of my research was also related to developing a methodology for estimating wave conditions at unmonitored coastal sites in the Hawaiian Island and in reef-fringed island

regions. Based on a linear numerical model, wave height predictions will be compared with the field measurements. This is described in chapter 3.

Because I started working on both projects, while these projects had already started, an extensive description of these projects is given in order to give a complete overview of the projects. If the reader is interested, she/he can contact the Department of Ocean Engineering at the University of Hawaii at Manoa to get the latest information on both projects.

The views expressed in this report are my views and do not necessarily reflect the views of other participating researchers.

## **2. Refraction-diffraction nonlinear waves**

### **2.1 Project description**

In order to capture the 'big picture' of this project, an extensive description is given consisting out of the rationale, some background information, the problem definition, the goals and objectives and the used research methods and approach.

#### **2.1.1. Rationale**

The action of waves has an important effect on coastal morphology. Waves erode beaches and damage coral reefs and other marine habitats. To determine the effects of this wave action on coastal areas, it is necessary to accurately monitor the wave climate. It is not economically feasible, however, to directly monitor a large number of nearshore sites. Hence, it is essential to develop accurate theoretical and numerical models to predict this wave action. The usual approach to predict waves in the nearshore is to drive linear refraction-diffraction models (as is used in chapter 3) with offshore measurements of directional wave spectra. These models are limited by the assumption of linearity which often is not valid in shallow waters. Therefore, it is necessary to develop models that simulate nonlinear directional random waves moving over an irregular sea floor in finite water depth.

#### **2.1.2. Background**

The majority of the refraction-diffraction models currently in use are based on the work of Berkhoff (1976) who derived an elliptic equation describing the wave transformation process. This equation, also known as the mild-slope equation, later was simplified by further assuming that the diffractive effects in the direction of wave propagation are small. This led to the so-called parabolic approximation, Radder (1979) which was extended to a higher-order by Kirby (1986). A variation of the parabolic wave-transformation equation is solved numerically by Ebersole (1985). This model has since

become a standard in such calculations although extensions of the past theoretical and numerical works on the subject are being pursued currently (e.g. Pan Chang and Pearce, 1991; Massel, 1993) to decrease the errors that result from the simplifying assumptions made (such as the slowly varying sea floor).

### **2.1.3. Problem identification**

Wave transformation in the nearshore must capture both refraction and diffraction effects. The models that are based on refraction only (c.f. Longuet-Higgins, 1957) may be particularly inadequate in the unique Pacific-basin island environment, because significant diffraction occurs. The models that are based on linear theory for monochromatic or random waves can be used in general; however, these models cannot capture the nonlinear wave-wave interactions in finite-water depth. Thus, errors are expected in predicting, for example, particle excursions which must be accurately calculated especially in problems related to sediment transport and the resulting beach erosion. The importance of nonlinearity has been demonstrated by Elgar et al. (1993) who observed the shoaling of directionally spread nonlinear waves.

Wave speed, particle velocities and accelerations and wave elevation all are affected by steep bottom slopes and nonlinear effects. Linear theory cannot predict the particle excursions, velocities and accelerations above the still-water level, because waves are assumed infinitesimally small in the theory. Therefore, it is necessary to develop a theoretical-numerical model that can accommodate the nonlinear and topographic effects in the wave transformation process. It is this process that the present project addresses by using a set of nonlinear water-wave equations in finite depth to model irregular, directionally spread waves.

### **2.1.4 Goals and objectives**

The overall goal of this project is to develop computational capabilities to predict the refraction and diffraction of nonlinear, directional random waves in the nearshore environment. To attain this goal, the following objectives are pursued sequentially:

- i) Waves that propagate in two horizontal dimensions over realistic bottom topography in relatively deep and shallow water will be modeled with the nonlinear Green-Naghdi equations (see paragraph 2.2). This study includes determining the accuracy of various levels of these equations when compared with experimental data in both deep and shallow waters. Determining the minimum required accuracy to simulate realistic wave transformation problems is very important because numerical simulations of the higher level Green-Naghdi equations are computationally demanding.
- ii) In conjunction with another project, which will be briefly discussed in chapter 3, the deep ocean wave characteristics, in terms of energy content and directionality, will be obtained. Available directional buoy measurements operated by the Army Corps of Engineers and others will be utilized to achieve this objective.
- iii) A three-dimensional numerical model will be developed to simulate the nonlinear random wave transformation as an unsteady process. This numerical model, based on the nonlinear wave equations of Green-Naghdi, will use the offshore wave measurements as input. As the measurements only will be obtained at a limited number of sites, it is initially assumed that the wave properties vary slowly over the entrance boundary of the model. Further refinement of this assumption will include using model results from the other project as input. The simulations also will use the digitized bathymetry charts to incorporate the effects of bottom irregularity. The numerical model will be based on the time marching of nonlinear evolution equations, and will be able to predict both the regular (monochromatic) and irregular wave transformations in short- or long-crested (swell) waves.

### **2.1.5 Research methods/approach**

The literature on wave transformation in the nearshore recently has been reviewed by Hamm et al. (1993) and Mei & Liu (1993). These works are referred to for references on many different aspects of wave transformation in the coastal zone, including wave breaking and dissipation mechanisms which may have a significant impact on the wave dynamics in very shallow waters. While wave run-up and run-down is important, this

current study addresses wave motion driven by inertia and gravity forces. Then, the typical approach to model wave transformation is to use the ideal flow assumption and to incorporate energy dissipation sources by empirical methods. This approximate approach currently is used due to the inability to model and solve the exact mathematical equations of physics. Another major problem is the enormous computational resources required when large-scale intensive computations must be done to solve the physical problem.

Although the ideal flow equations, namely the Laplace equation subject to the free-surface and sea floor boundary conditions, are well established, their numerical solutions are difficult to obtain due to the nonlinear boundary conditions. Some small-scale problems both in two- and three-dimensions using the exact equations have been solved only recently using the boundary-element method (c.f., Chian & Ertekin, 1992; Yang & Ertekin, 1992). The large-scale problems extending, for example, from 1 km to 10 km in the horizontal plane, cannot be solved by such methods. Therefore, it is essential to use equations that can capture most of the physics of the problem. Liu et al. (1985) attempted to do this in shallow waters by using the Boussinesq equations in two-dimensions (vertical plane). As they invoked the parabolic approximation which is confined to a small-angle of diffraction, the usefulness of their approach is limited in practical problems.

## **2.2 Green-Naghdi equations**

The general derivation of the G-N equations is lengthy and I refer the reader to selected references (Shields and Webster, 1988; Demirbilek and Webster, 1992a) for details. Briefly, Green and Naghdi (1976) developed a theory of directed fluid sheets in which the kinematic and dynamic boundary conditions and the continuity equation are satisfied exactly. The conservation of momentum, however, is satisfied by using a vertical weighted average.

There are different Levels of Green-Naghdi equations, where for our purposes the difference between the levels refers to the assumed form of the velocity variation in the vertical direction across the fluid sheet. In Ertekin and Becker (1996), the 2-D G-N Level I equations are used, where Level I refers to the horizontal velocity in the x-direction, i.e.,  $u(x,t)$ , is depth independent and the vertical velocity is a linear function of the vertical coordinate,  $z$ . The 2-D G-N Level I equations are given by (e.g., Ertekin, 1984, 1988):

$$D\eta + (\eta + h)u_x + uh_x = 0 \quad (1)$$

$$Du + g\eta_x = -\frac{1}{6}\{(4\eta + h)_x D^2\eta - (2\eta - h)_x D^2h + (\eta + h)(2D^2\eta - D^2h)_x\} \quad (2)$$

where  $u$  is the horizontal particle velocity vector and  $D$  is the 1-D material time derivative

$$\text{operator } D = \frac{\partial}{\partial t} + u \frac{\partial}{\partial x} \quad (3)$$

and  $D^2 = DD$ , is the second material time derivative. The Level I G-N equations also have been used by Ertekin and Wehausen (1986) to study the diffraction of solitary waves over a shelf.

In Shields and Webster (1988), a comparison between different G-N theories (Level I, II and III) and the exact solution for the dispersion relation for infinitesimal waves is made. From this comparison, it is possible to obtain an indication of the range of validity of  $\lambda/h$  for a specific G-N theory. Based on their findings the G-N Level II equations should provide acceptable results for  $\lambda/h > 5$  and the G-N Level I equations for  $\lambda/h > 8$ . As will be shown, it is the shortest wave length that corresponds to the highest harmonic generated when a finite-amplitude wave encounters a topography change that must lie in the range for which linear dispersion is accurately modeled. This means that if the experiments show a significant amount of energy in a certain higher harmonic and the corresponding ratio of the wave length over the water depth is outside the validity range,

the higher harmonic will not be picked up by the model and the accuracy of the simulation will be degraded.

The Level II G-N equations are based on the same dynamics as Eqs. (1) and (2), but the horizontal particle velocity  $u(x,z,t)$  and the vertical velocity  $w(x,z,t)$  are expressed as:

$$u(x, z, t) = u_0(x, t) + u_1(x, t) z \quad (4)$$

$$w(x, z, t) = w_0(x, t) + w_1(x, t) z + w_2(x, t) z^2 \quad (5)$$

Again the boundary conditions and the 3-D continuity equation are satisfied exactly, and the 3-D momentum conservation is satisfied approximately. The G-N Level II equations over a variable bathymetry consist of three equations for  $\eta$ ,  $u_0$  and  $u_1$ . These may be found in Shields (1986) and Demirbilek and Webster (1992a).

### 2.3 ANALYSIS

The program GNWAVE, developed by Demirbilek and Webster (1992b), is used for the calculations. It is based on the 2D G-N Level II equations over a variable bathymetry and can be used for a  $\lambda/h$  ratio between 2.5 and 100, where  $\lambda$  and  $h$  are the wave length and the water depth at the wave maker in the case of monochromatic sinusoidal waves. As input, the horizontal extent of the computational domain, the maximum calculation time, the bottom profile, the wave height and wave period are needed. GNWAVE determines the amplitude of the wave ( $\eta$ ) above the undisturbed free surface, the horizontal velocity components  $u_0$  and  $u_1$ , the pressure measured at a user-defined depth, the integrated pressure (integrated from the bottom to the actual water surface) and the first moment of the pressure (pressure multiplied by the vertical coordinate and integrated from the bottom to the actual water surface) as a function of the spatial coordinate and time. The spatial resolution  $\Delta x$  used in GNWAVE equals  $1/100^{\text{th}}$  of the incident wave length at the wave maker and the time step  $\Delta t$  equals  $1/100^{\text{th}}$  of the incident wave period.



The flow near the wave maker and near the right-hand boundary suffers from an alternate point instability that may result in high and low oscillations of the three independent variables ( $\eta$ ,  $u_0$  and  $u_1$ ) at neighboring points on the finite difference grid. In GNWAVE, this is corrected by smoothing the first few and the last few points in the computational domain. During our calculations, it was necessary to alter the existing filtering, because the waves were breaking over the shelf. The filter which is used for these calculations is given by (Shapiro (1975)):

$$f(i) = \frac{1}{16} [10 f(i) + 4\{f(i+1) + f(i-1)\} - \{f(i+2) + f(i-2)\}] \quad (6)$$

where  $f(i)$  refers to either the surface elevation or the velocity components in the computational domain. This filter is applied at every five time steps in order not to over-filter the results.

## 2.4. Results

### 2.4.1. Set up # 1

The first numerical set up corresponds to the wave tank used in Ohyama et al (1995) and is given in Fig. 2, where all distances are made dimensionless using  $h_0$ , where  $h_0$  is the water depth at the wave maker ( $h_0 = 0.5$  m). The wave maker is located at the left end of the numerical wave tank, at the right end there is an open boundary and at five different locations, numerical wave gages are placed which record the surface elevation as a function of time.

In this paper, three selected cases are presented for which the wave parameters are presented in Table 1 (the case numbers correspond to Ohyama et al., 1995). The objective of this numerical experiment is to compare the G-N Level II results with experimental

data and to compare the results of the G-N Level II equations with the results of the G-N Level I equations (Ertekin and Becker, 1996).

Case #	Period $T\sqrt{g/h_o}$	Length $\lambda/h_o$	Height $H/h_o$	$H/\lambda$
2	5.95	4.72	0.1	0.0212
4	8.92	8.16	0.1	0.0123
6	11.88	11.35	0.1	0.0088

Table 1 Wave parameters used in the calculations for set-up #1

In the Figs. 3a-f, the dimensionless surface elevation as a function of the dimensionless time are shown for the three different cases at two different locations (at gages 3 and 5, see Fig. 2). The time series are shifted to fit the peak of the wave elevation in the calculations to the peak of the wave elevation in the experimental data. From these figures it can be seen that the G-N Level II equations simulate the experimental data better than the G-N Level I equations in particularly modeling the higher harmonics that occur when finite-amplitude waves propagate over the steep shelf. In fact, the G-N II equations exhibit almost all of the higher harmonics that were observed during the experiments. They predict the general location and the amplitude of the surface elevation peaks better. In general, the predictions of the surface elevation are better in front of the shelf than behind the shelf, where energy is transferred to higher harmonics.

The Level II G-N equations provide a good prediction of the surface elevation at station 3 for case 2, although, as with the Level I G-N equations, the wave elevation is slightly underestimated. A spectral analysis of the experimental data shows that only the first and second harmonics are of importance at this station, and  $\lambda/h$  equals 4.2 at this station, based on the wave length of the second harmonic. That the Level II G-N equations do better than the Level I G-N equations confirms what we expect from the work of Shields and Webster (1988), which shows that the G-N Level II and G-N Level I equations describe the linear dispersion relation well for  $\lambda/h > 5$  and for  $\lambda/h > 8$  respectively. In

short, the Level II G-N equations do a better job at modeling the second harmonic at station 3.

For case 2 at station 5, a spectral analysis of the experimental data (Fig. 4a indicates that the first harmonic is most energetic and that the second and third harmonics are excited. A spectral analysis of the numerical results (Fig. 4b however, show that the third harmonic is not modeled well, which is consistent with the corresponding  $\lambda/h$  ratio ( $\lambda/h = 0.6$ ) lying well outside the range of validity of the linear dispersion relationship for both models. In addition, in the G-N Level II solution, the second harmonic contains more energy than the first harmonic. A similar overestimation of the energy in the second harmonic is seen in a numerical solution of the Stokes second-order model (Ohyama et al., 1995 figure 7), where the third harmonic is not taken into account.

Cases 4 and 6 correspond to longer and less nonlinear waves than those of case 2, but the accuracy of the G-N Level II predictions still depends upon how well the highest harmonic generated is modeled. For cases 4 and 6 at station 3, the G-N Level II equations model the wave height well. The highest harmonics excited at this station correspond to  $\lambda/h = 2.6$  and  $4.2$  for cases 4 and 6, respectively, so any discrepancies are likely due to the  $\lambda/h$  ratios being just outside the limit of the range of validity.

For case 4 at station 5, a spectral analysis of the experimental data (Fig. 4c) shows the third harmonic is dominant. In contrast, the first harmonic dominates the numerical data (Fig. 4d) as the third harmonic ( $\lambda/h = 1.4$ ) is too short to be modeled accurately. For case 6 at station 5, the energy in the fourth harmonic is significant and the corresponding ratio of  $\lambda/h$  equals 1.4. So it is expected and confirmed in the spectral analysis (compare Fig. 4e and 4f) that the model cannot capture this harmonic very well. That the G-N Level I equations provide less accurate predictions than the G-N Level II equations for these experiments is expected, because the G-N Level I equations are accurate only for longer waves.

### 2.4.2. Set up # 2

The second numerical set up corresponds to the wave tank used Ohyama et al. (1994), and is given in Fig. 5a. In the experiments, a plane beach with coarse material was placed as a wave absorber at the right end of the wave tank. In our calculations, this is modeled as an open boundary (see Fig. 5b). Two monochromatic wave cases are studied for which the corresponding wave parameters are presented in Table 2, where  $h_0$  is the water depth at the wave maker ( $h_0 = 0.4$  m).

Incident waves	Period $T\sqrt{g/h_0}$	Wave height $H/h_0$	Length $\lambda/h_0$	$H/\lambda$
long	9.90	0.05	9.24	0.005
short	6.19	0.0625	5.13	0.012

Table 2 Wave parameters used in the calculations for set-up #2

The initial wave height for the short wave case is larger, because it was attempted to keep the nonlinearity parameter, i.e., the wave amplitude/water depth ratio, almost the same in the shallowest region of the tank.

In the Figs. 6a-g the dimensionless results for the long monochromatic wave case at the different wave gages are shown, where the numerical results after 10 periods from the cold start have been used. As can be seen from these figures, the numerical data agree well with the experimental data in front of and over the submerged bar. As the end of the bar is reached, the agreement between the numerical simulations and the experimental data is less satisfactory, but the model is still able to pick up almost all the higher harmonics which occur.

The results for the short monochromatic wave case, 20 periods from the cold start, are presented in the Figs. 7a-d. For this case, the numerical and experimental data agree well

for all the stations. It might be expected that the long wave case should give better results than the short wave case, because the  $\lambda/h$  ratio will be larger (based on the incident wave length), but as is mentioned in Beji and Battjes (1992), higher harmonics occur due to resonant interactions in the long wave case. These higher harmonics cannot be predicted accurately here, as they exceed the  $\lambda/h$  range of validity, which give discrepancies between the experimental and numerical data.

## 2.5 Discussion

The Green-Naghdi Level II equations are used to determine the diffraction of nonlinear waves by a submerged shelf. Two different numerical set ups are investigated and for each set up, the numerical solutions are compared with the experimental data of Ohyama et al. (1994) and Ohyama et al. (1995). For the monochromatic waves, the G-N Level II equations showed a very good agreement in front of and over the shelf. The results of the G-N Level II equations behind the shelf provide better predictions than the G-N Level I equations, because the higher harmonics are modeled more accurately.

Considering the long wave case versus the short wave case over the gradual shelf, an interesting phenomenon is observed. One would expect the G-N Level II equations to predict the long wave case better, because the  $\lambda/h$  ratio is larger, but at the same time higher harmonics, due to resonant interactions, become more important. If the corresponding ratio of  $\lambda/h$  of the highest harmonic, which is still of importance, lies outside the range of validity, the predictions will be less accurate. In this case, the trade off between more accuracy due to longer waves and less accuracy due to higher harmonics is such that the short wave case predicts the wave heights better.

### **3. Linear wave model verification**

#### **3.1 Project description**

During the summer of 1996 I worked on another project as well. The description of that project is given in the following paragraphs.

##### **3.1.1. Rationale**

The modeling of wave transformations due to variable bathymetry has received considerable attention in recent decades (see Mei and Liu, 1993 for a review). Linear numerical models that account for wave refraction and diffraction have been shown to simulate wave properties at a variety of coastal settings (c.f., O'Reilly and Guza, 1993). In practice, measurements of directional wave spectra in the deep ocean can be transformed numerically into corresponding coastal wave spectra. This simple modeling approach provides cost-effective means of assessing the impact of waves at unmonitored sites. The coastal wave database is essential for beach erosion and replenishment, the mitigation of wave damage caused by hurricanes and tropical storms, and the establishment of setbacks for coastal development.

Coastal wave prediction in the Hawaiian Island region has been limited until recently by the lack of deep ocean directional wave data. The four NOAA (National Oceanic and Atmospheric Administration) wave buoys (Fig. 8) measure wave energy but not direction. Recently, the Army Corps of Engineers (CE), the State Department of Transportation (DOT) and the US Navy (USN) have proposed the expansion of the existing deep water wave gage network around Hawaii to include directional wave buoys. Wave conditions at unmonitored coastal sites could then be predicted from a limited number of offshore buoys using transformation models. This program would satisfy the demand for wave climate data as well as short-range wave forecasts. An improved wave prediction capability for the region has drawn strong support from the State Department of Civil Defense, Transportation, Land and Natural Resources, the Coastal Zone

Management Program of the Office of State Planning, the National Weather Service and local ocean engineering firms.

A key issue to be addressed prior to the expansion of the wave gage network is the expected accuracy of the coastal wave estimates. O'Reilly and Guza (1991) note that while linear transformation models and buoy data can produce realistic estimates of wave properties in regions of complex topography, model performances tend to be site-specific depending on the local bathymetry and deep water wave characteristics. Specifically, the application of wave models that have been developed for wide, gently slope continental shelves may not be entirely appropriate for the Hawaiian Island region where fringing reef systems, steep bathymetric slopes and neighbor island sheltering effects are present.

A second issue specific to island regions is how well coastal waves can be estimated shoreward of fringing reefs. Once waves break at offshore reefs, the linear refraction/diffraction models no longer apply. Wave reformation may occur shoreward of the reefs (c.f., Gerritsen, 1980, 1981), however, and here linear models may again prove useful in estimating wave transformations towards shore.

The combination of this project with the one described in chapter 2 is very important in that linear refraction-diffraction models provide useful results for wave propagation when the topography is slowly-varying and outside the nearshore. As waves shoal or encounter abrupt topographic features, however, linear models are no longer adequate and finite-amplitude effects must be incorporated. So it is necessary to find out until what water depths the linear models are still applicable and at what water depths nonlinear models have to be used. It is very advantageous if the linear models would describe the wave transformation accurately as close to the shore as possible, because these models are computationally very efficient compared with the nonlinear models.

### **3.1.2. Goals and objective**

The primary goal of this project is to develop a methodology for estimating wave conditions at unmonitored coastal sites around the Hawaiian Islands specifically, but for reef-fringed islands in general. A field experiment is proposed consisting of an array of directional and non-directional wave gages that will be deployed in intermediate water

depths (3-30 m) at various locations around the island of Oahu (Fig. 1). Two main deployments will be made during the winter to measure wave conditions associated with North Pacific swell and northeast trade winds and during the summer to measure swell originating from the Southern Hemisphere and waves generated by local tropical storms and hurricanes (Fig. 9). The summer deployment will also provide information on wave wrap-around effects as Northeasterly trade wind-driven waves, which are at an annual maximum, often arrive at the south-facing beaches at oblique angles.

The specific goals that will be addressed include:

- i) The accuracy and precision of the model simulations as a function of dominant wave direction, wave height and frequency, season and location. In particular, the ability of the linear models to predict large wave conditions at the coast due to local and remote storm events.
- ii) The empirical relationship between deep water and reformed waves shoreward of reefs.
- iii) The performance of the transformation models offshore and shoreward of reefs.
- iv) The accuracy of wave model estimates for sites where island sheltering is important.
- v) The relative merits of refraction versus refraction/diffraction models as applied to island regions with complex reef systems. Model verification will provide insight into whether refraction/diffraction models, which are considerably more intensive computationally than refraction models, are necessary.
- vi) The accuracy of the predictions near regions of steep topography where the mild-slope assumptions for parabolic equation refraction/diffraction models are violated.

A practical objective of this study is to build a database of coastal measurements and model predictions that can be utilized for management, planning and research purposes. Wave transformation coefficients for specific sites will be made available to compute shallow water spectra from offshore measurements of the wave field. To address the specific needs of the State Civil Defense Department the feasibility of making real-time predictions of wave height and direction that can be used for disaster response purposes will be examined.



### 3.1.3. Research methods/approach

The project is divided into two major tasks: (1) the collection of wave data for both winter and summer conditions in representative topographic settings around the island of Oahu, and (2) the modeling of wave transformations using offshore buoy data and linear wave models the results of which will be compared with observations. The former requires the deployment and recovery of battery powered instrument systems, while the latter involves the establishment of an appropriate model grid and the acquisition and implementation of refraction and refraction/diffraction models. The specific methods and approach are outlined below.

#### Field Measurements

To measure wave energy at the coast (non-directional), 4 pressure sensors developed at the Scripps Institution of Oceanography will be used. The instrument packages contain a pressure sensor (Setra Model 280E), battery, and 20 mbyte internal hard disk. Sampling at 1 hz, continuous data can be acquired for approximately 3 months. The continuous pressure data will provide high statistical stability for the wave estimates. The basic instrument design has been tested in a field experiment in the Southern Californnie Bight and has been found to measure surface waves with periods greater than 8 seconds in 25-35m total water depth.

In addition to the new instrumentation, a pressure recorder will be borrowed from Look Laboratories (laboratories of the Department of Ocean Engineering) for both deployments, and data from the waverider buoy at Makapu'u Point will be obtained from the Coastal Data Information Program (CDIP). The Makapu'u Point data will be particularly useful in that wave climatology has been well documented at this location by CDIP. The study will provide insights into the establishment of this wave climate. Directional wave data will be obtained using an Inter-Ocean S4A. The S4A contains an electromagnetic current meter, a Paroscientific pressure sensor, battery pack, and 20

mbyte internal memory. Sampling continuously at 1 hz, the sensor can collect data for approximately 40 days.

Burst sampling can increase the deployment length as required. In addition to directional wave estimates, the S4A will record current speed and direction which may prove useful for investigating wave-driven flows. In order to limit costs for the initial project, the instrument will be leased from Ecosystems in Carlsbad, CA. The accuracy and precision of the S4A will be tested in the Look ocean test range prior to deployment.

Two field experiments are planned. The first will take place during the winter on the windward coast of Oahu in order to measure waves generated by trade winds and northern storms.

The deep water directional wave buoy north of the island of Molokai (Fig. 1) will provide unsheltered estimates of the incoming waves associated with the northeast trade winds, and for most northern swell directions. In order to measure waves in a full range of locations, the sensors will be deployed in clusters at several different sites. This will require a number of dive expeditions in order to reposition the sensors. The redeployment of the sensors will allow for data recovery and analysis that will help in choosing subsequent deployment sites. The exact location of the experiments also will be chosen based on preliminary model simulation studies.

The second experiment will take place at south facing beaches that are exposed to summer storms. The deep water wave gage off of the island of Lanai (Fig. 1) will provide offshore wave spectra for model initialization. The objective of this experiment is to measure waves from distant summer storms in the southern hemisphere, and large amplitude waves due to local fronts or extra-tropical lows. Such conditions can lead to extremely large significant wave heights (Fig. 10).

Anticipated deployments include sensor arrays on a transect over a fringing reef, in the vicinity of a gap in the reef, at sheltered and unsheltered sites, shoreward of the steep island slope, and near embayments and headlands. The goal is to test the model simulations for a wide range of conditions that typify the island region. Typically, a deep water deployment (i.e., offshore of any reefs) will be made for comparison with the deep ocean wave gage spectra. In particular, the extent of local wind generated waves (i.e.,

between the deep water and coastal sensors) will be assessed. Instruments also will be placed on transects perpendicular to shore. Variations on the transect array will be made depending on local topographic conditions. The instrument array will be relocated after 1 or 2 month deployments to new sites. The length of the deployments should be sufficient to encounter a variety of incoming wave conditions.

### Numerical Modeling

The transformation of wave properties from deep to shallow water will be accomplished using both a spectral refraction model (Longuet-Higgins, 1957) and a combined refraction-diffraction model based on a parabolic equation method (Kirby, 1986). The refraction-diffraction model is currently being used by CDIP to model waves in the Southern California Bight (O'Reilly and Guza, 1993).

Although the refraction-diffraction model assumes that topographic slopes are mild, the model results have been found to be robust for some steep slope applications (O'Reilly, communication, 1994). Field verification of the model estimates is essential, however, before the numerical results are of practical use. An initial task will be the formation of a topographic model grid. The density of sounding data around the islands is highly uneven. In addition, reef location and geometry is often not well defined. Once study sites have been designated, supplementary sounding data will be collected to improve the raw data coverage.

### **3.2. Wave height predictions**

In order to be able to determine the wave heights for a particular location the model based on a parabolic equation method (Kirby, 1986) is used. The input for this program is the incident wave height, the wave period ( $P$ ) and the wave angle ( $\alpha$ ). This means that for each run the wave height for a single wave component only will be determined, see for example Fig. 11 and 12 where for two different locations (Waikiki beach and Kailua Bay, see Fig. 13) the wave height predictions are given for a wave period of 10 seconds and a

wave angle of 205° and 65° relative to North, respectively. These simulations are based on the bathymetries as shown in Fig. 14 and Fig. 15.

In order to simulate a directional wave spectrum  $S(\omega, \theta)$ , different wave periods and wave angles have to be taken into account, while the incident wave height is kept at 1 m. The actual prediction of the wave heights  $H(x, y)$ , due to this spectrum is obtained by summing the influence of each of the individual wave components  $H_i(x, y)$ . Based on the measured spectrum  $S(\omega, \theta)$ , a weight factor  $w_i(\omega, \theta)$  for these wave components can be obtained, which equals the contribution of that wave component to the total variance of the spectrum:

$$H(x, y) = \sum_{i=1}^n \sqrt{w_i(\omega, \theta)} H_i^2(x, y) \quad (7)$$

$$\sum_{i=1}^n w_i(\omega, \theta) = \iint_{\omega \theta} S(\omega, \theta) d\omega d\theta \quad (8)$$

In Fig. 16 the prediction of the wave heights is shown for Waikiki when the wave period ranges from 8 until 20 seconds with an increment of 2 seconds and the wave angle ranges from 185° until 265° with an increment of 10°. For this case a hypothetical spectrum is assumed with a significant wave height of 2 meters, and a normal distribution with  $\mu_p = 14$  s,  $\sigma_p = 4.32$  s,  $\mu_\alpha = 175^\circ$  and  $\sigma_\alpha = 27.39^\circ$ .

In Fig. 17 the same is shown for Kailua Bay, where the wave period range is kept the same and the wave angle ranges from 55° until 85° with an increment of 10°. For this case the same hypothetical spectrum is assumed with  $\mu_p = 14$  s,  $\sigma_p = 4.32$  s,  $\mu_\alpha = 70^\circ$  and  $\sigma_\alpha = 11.18^\circ$ .

As can be seen from these figures, there are a couple of locations where the wave height is significantly increased (so called hot spots). At these locations the wave gages are deployed and the obtained field data will be compared with the model predictions in order to check the validity of the used computer model.

#### 4. References

- Beji S. and Battjes J.A. (1992), "Experimental Investigation of Wave Propagation Over a Bar", *Coastal Engineering.*, Vol. 19, pp. 151-162.
- Berkhoff J.C.W. (1973), "Computation of Combined Refraction-Diffraction", *Proc. 13<sup>th</sup> Intl Conf. on Coastal Engineering*, Vancouver, Canada, ASCE, pp. 471-490.
- Berkhoff J.C.W. (1976), "Mathematical Models for Simple Harmonic Linear Water Waves, Wave Diffraction and Refraction", Delft Hydraulics Lab., Pub. No. 163, The Netherlands, April
- Chamberlain P.G., Porter D. (1995a), "The Modified Mild-Slope Equation", *J. Fluid Mech.* 291, pp. 393-407.
- Chian C. and Ertekin R.C. (1992), "Diffraction of Solitary Waves by Submerged Horizontal Cylinders", *Wave Motion*, 15(2), pp. 121-142.
- Demirbilek Z., Webster W.C. (1992a), "Application of the Green-Naghdi Theory of Fluid Sheets to Shallow-Water Wave Problems", U.S. Army Corps. of Eng. Waterways Experiment Station, Rep. No. CERC-92-11, Vicksburg, MS.
- Demirbilek Z., Webster W.C. (1992b), "User's Manual and Examples for GNWAVE" U.S. Army Corps. of Eng. Waterways Experiment Station, Rep. No. CERC-92-11, Vicksburg, MS.
- Ebersole B.A. (1985), "Refraction-Diffraction Model for Linear Water Waves", *J. Waterway, Port, Coastal and Ocean Eng.*, 111(6), pp. 939-953.
- Elgar S., Guza R.T. and Freilich M.H. (1993), "Observation of Nonlinear Interactions in Directionally Spread Shoaling Surface Gravity Waves", *J. Geophys. Research* 98, pp. 20,299-20,305.
- Ertekin R.C. (1984), "Soliton Generation by Moving Disturbances in Shallow Water: Theory, Computation and Experiment", Ph.D. Dissertation, U.C. Berkeley, May, v+352 pp.
- Ertekin R.C. and Wehausen J.V. (1986), "Some Soliton Calculations", *Proc. 16<sup>th</sup> Symp. On Naval Hydrodynamics*, Berkeley, July, pp. 167-184, Disc. P. 185 (Ed. by W.C. Webster, National Academy Press, Washington, D.C., 1987).

- Ertekin R.C. (1988), "Nonlinear Shallow Water Waves: The Green-Naghdi Equations", *Proc. Pacific Congress on Marine Sci. & Techno.*, PACON '88, Honolulu, May, pp. OST6/42-52.
- Ertekin R.C., Becker J.M. (1996), "Nonlinear Diffraction of Waves By a Submerged Shelf in Shallow Water", *Proc. of 15<sup>th</sup> Intl Conf. on Offshore Mechanics and Arctic Engineering*, ASME, June 16-20, Florence, Italy. In review, *J. Offshore Mech. And Arctic Engng.*
- Fletcher C.H. and Hwang D.J. (1994), "Shoreline Certification Review and Recommendations", a report to the Office of State Planning, Coastal Zone Management Program, in review.
- Freilich M.H., Guza R.T. (1984), "Nonlinear Effects on Shoaling Surface Gravity Waves", *Phil. Trans. R. Soc. Land.*, A311, pp. 1-41.
- Gerritsen F. (1980), "Wave Attenuation and Wave Set-Up on a Coastal Reef", *Proc. 17<sup>th</sup> Int. Conf. Coastal Engng.*, pp. 444-461.
- Gerritsen F. (1981), "Wave Attenuation and Wave Set-Up on a Coastal Reef", Look Lab. Tech. Rep. 48, pp.416.
- Green A.E., Naghdi P.M. (1976), "Direct Fluid Sheets", *Proc. Roy. Soc. London, Series A*, Vol. 347, pp. 447-473.
- Hamm L., Madsen P.A. and Peregrine D.H. (1993), "Wave Transformation in the Nearshore Zone: a Review", *Coastal Engineering*, 21, pp. 5-39.
- Kirby J.T. (1986), "Higher-order Approximation in the Parabolic Equation Method for Water Waves", *J. of Geophys. Res.* 91(C1), pp. 933-953.
- Kirby J.T. (1986), "A General Wave Equation for Waves over Rippled Beds", *J. Fluid Mech.* 162, pp. 171-186.
- Liu P.F., Soon S.B., Kirby J.T. (1985), "Nonlinear Refraction-Diffraction of Waves in Shallow Water", *J. Fluid Mech.* 153, pp. 185-201
- Longuet-Higgins M.S. (1957), "On the Transformation of a Continuous Spectrum by Refraction", *Proc. Cambridge Philos. Soc.* 53(1), pp. 226-229.
- Massel S.R. (1993), "Extended Refraction-Diffraction Equation for Surface Waves", *Coastal Engineering*, 19, pp. 97-126.

- Mei C.C. and Liu P.F. (1993), "Surface Waves and Coastal Dynamics", *Ann. Rev. Fluid Mech.* 25, pp. 215-240.
- Ohyama T., Beji S., Nadaoka K., Battjes J.A. (1994), "Experimental Verification of Numerical Model for Nonlinear Wave Evolutions", *J. of Waterway, Port, Coastal and Ocean Engineering*, Vol. 20, No. 6, November/December '94.
- Ohyama T., Kioka W., Tada A. (1995), "Applicability of Numerical Models to Nonlinear Dispersive Waves", *Coastal Engineering*, Vol. 24, pp. 275-296.
- O'Reilly W.C. and Guza R.T. (1991), "Comparison of Spectral Refraction and Refraction-Diffraction Wave Models", *J. Waterway, Port, Coastal Ocean Eng.* 117(3), pp. 119-125.
- O'Reilly W.C. and Guza R.T. (1993), "A Comparison of Two Spectral Wave Models in the Southern California Bight.", *Coastal Eng.* 19, pp. 263-282.
- Pan Chang V.G. and Pearce B.R. (1991), "Solution of the Mild-Slope Wave Problem by Iteration", *Applied Ocean Research* 13(4), pp. 187-199.
- Radder A.C. (1979), "On the Parabolic Equation Method for Water-Wave Propagation", *J. Fluid Mech.* 95, pp. 159-176.
- Shapiro R. (1975), "Linear Filtering", *Maths Comput*, Vol. 29, pp. 1094-1097
- Shields J.J. (1986), "A Direct Theory for Waves Approaching a Beach", Ph.D. thesis, University of California, Berkeley, iii+137 pp.
- Shields J.J., Webster W.C. (1988), "On Direct Methods in Water-Wave Theory", *J. Fluid Mech.* (1988), vol. 197, pp. 171-199.
- Yang C. and Ertekin R.C. (1992), "Numerical Simulation of Nonlinear Wave Diffraction by a Vertical Cylinder", *J. Offshore Mech. And Arctic Eng.* 114(1), pp. 34-44.

## 5. Figures





Figure 1 The Hawaiian Islands (degrees North and degrees West)

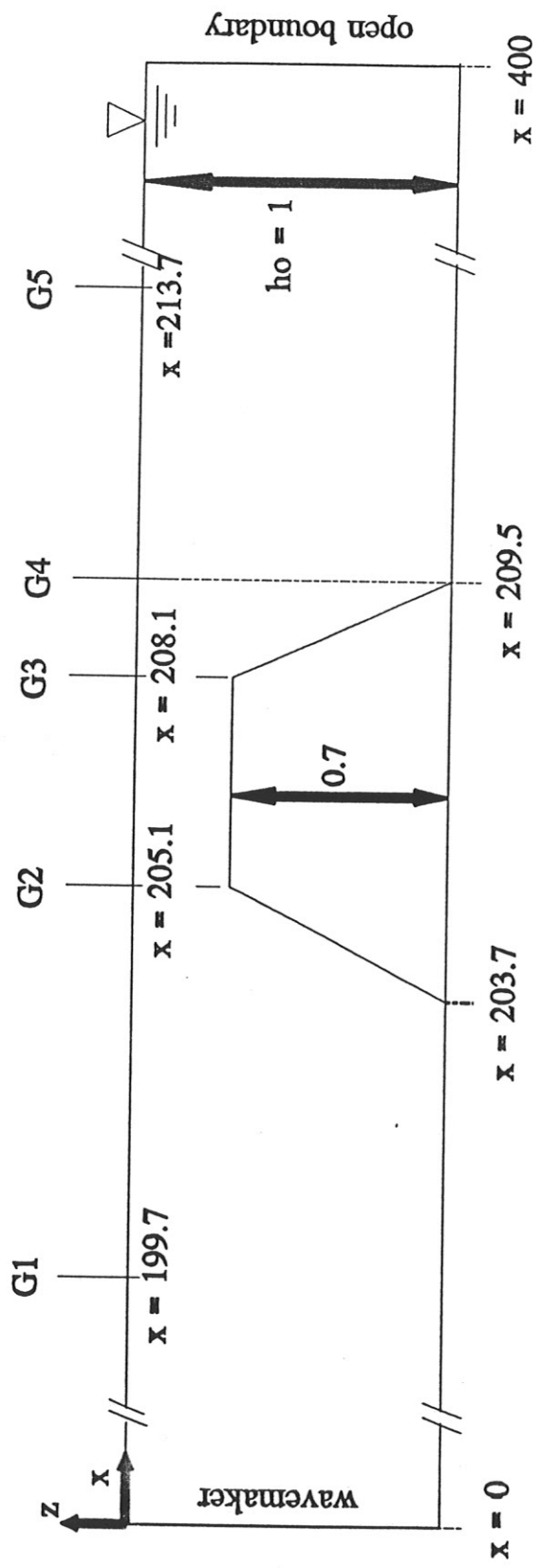


Figure 2 A schematic of the numerical wave tank used in Ertekin and Becker, 1996

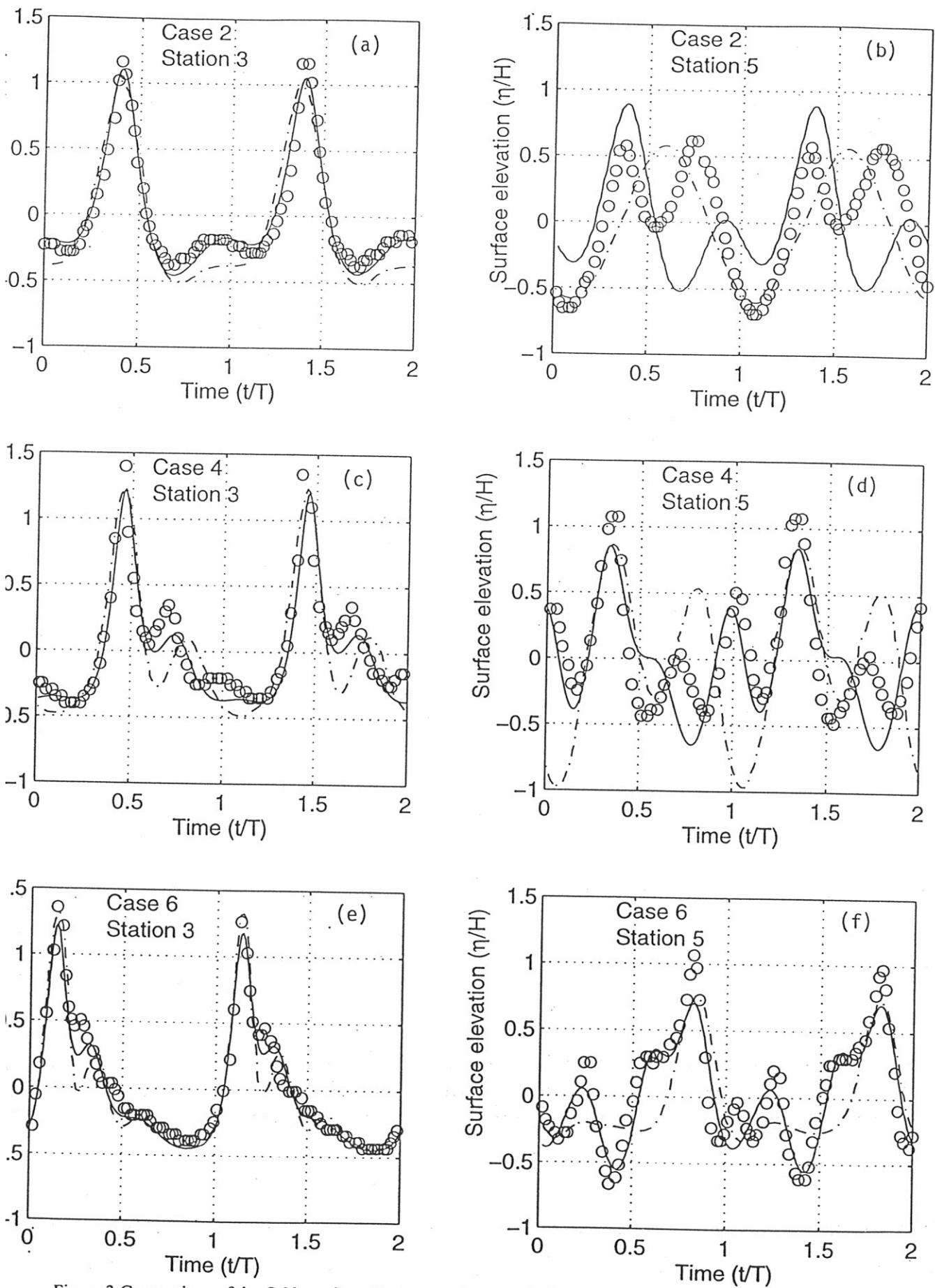


Figure 3 Comparison of the G-N results with the experiments of Ohyama et al. (1995) at wave gage G3 and G5. The free surface elevation,  $\eta/H$  as a function of time  $t/T$  for the following cases: (a) 2 at G3, (b) 2 at G5, (c) 4 at G3, (d) 4 at G5, (e) 6 at G3 and (f) 6 at G5. The circles refer to the experimental data of Ohyama et al. (1995), the solid line is the G-N II result and the dot-dash line is the G-N I result.

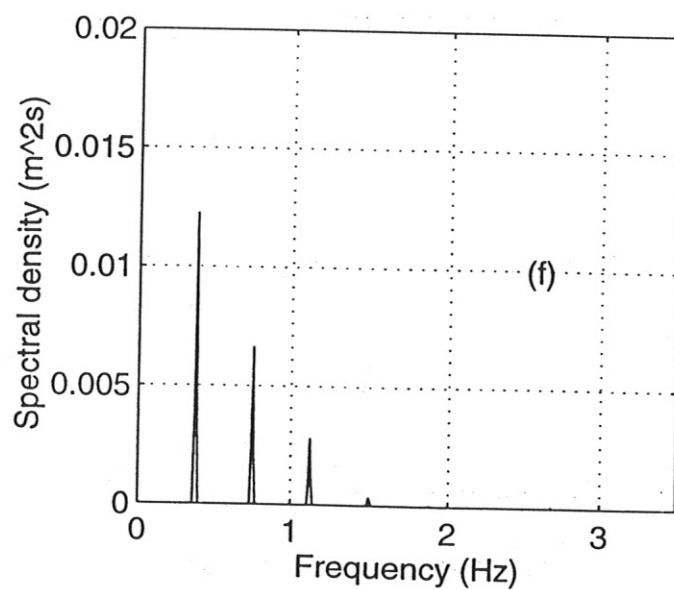
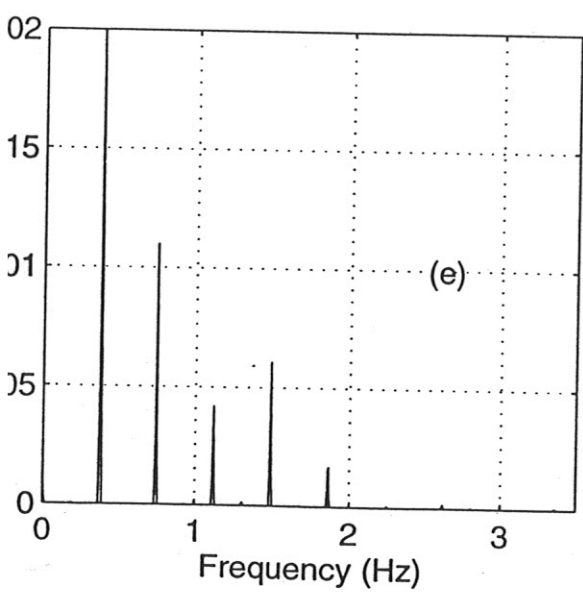
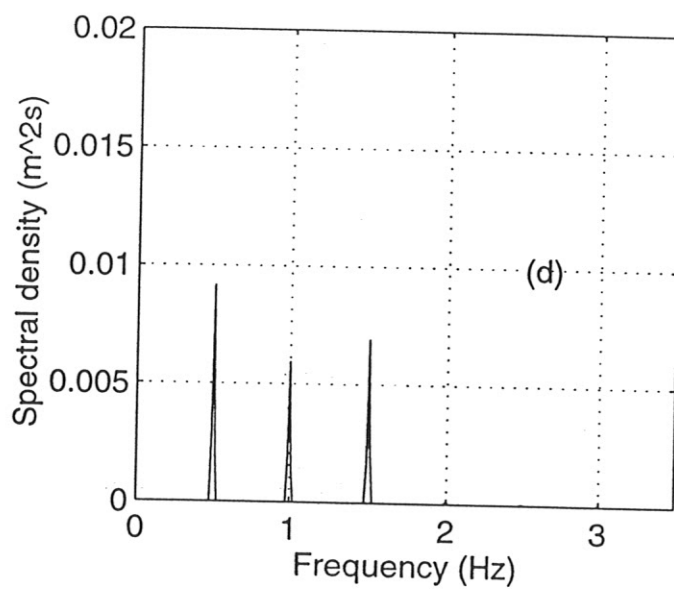
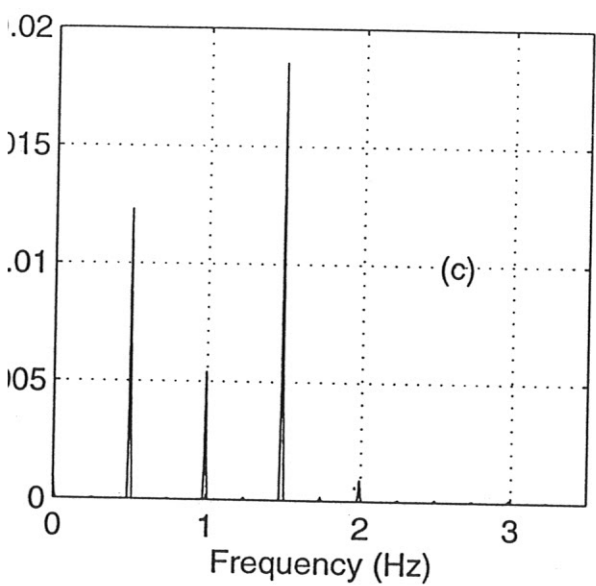
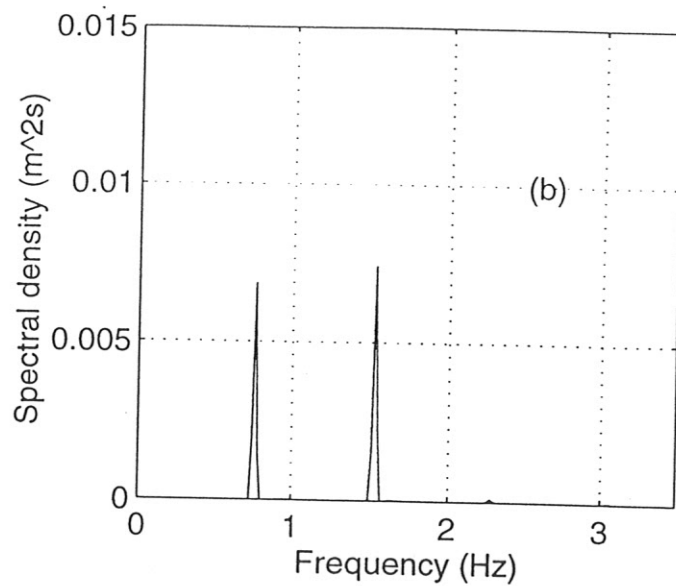
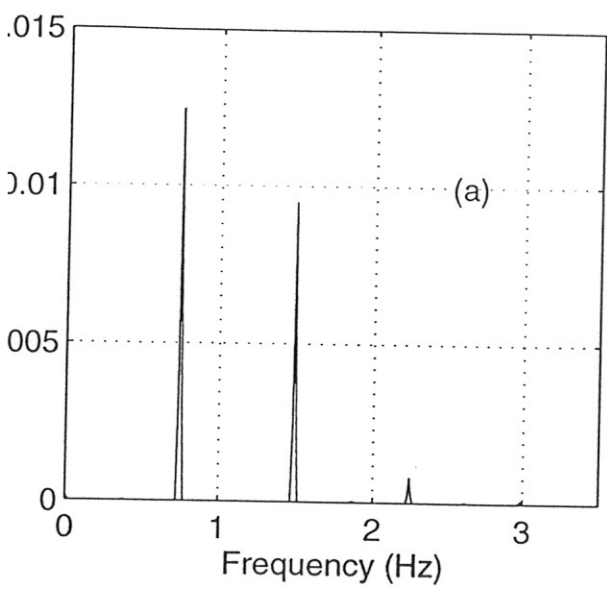


Figure 4 Spectral analysis of the experimental data (a, c, e) and the computer simulations (b, d, f) at wave gage 5 for case 2 (a) and (b), case 4 (c) and (d) and case 6 (e) and (f)

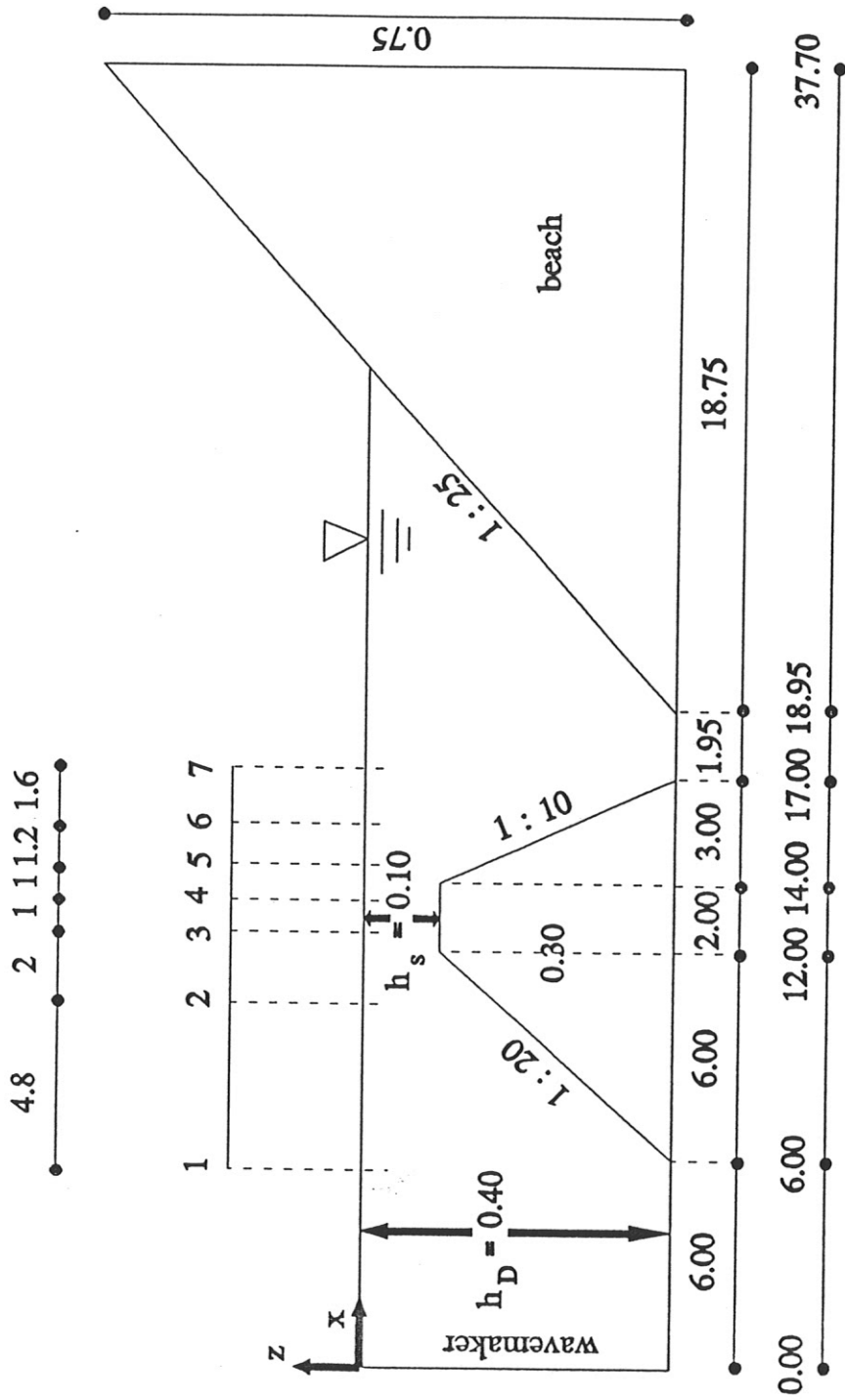


Figure 5a Schematic of the wave flume and the submerged bar used in the experiments of Ohyama et al (1994). All distances in meters.

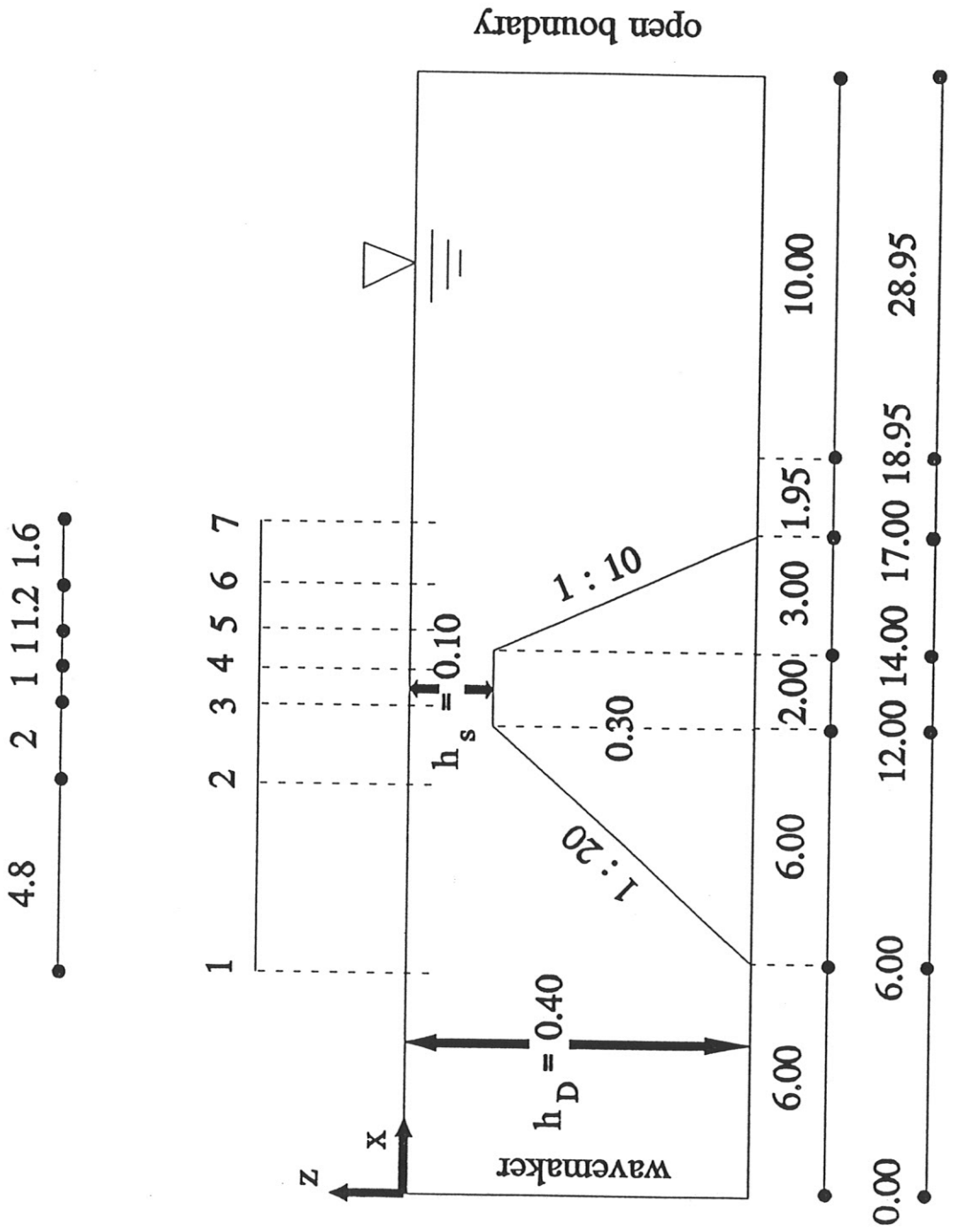


Figure 5b A schematic of the numerical wave tank, modeling figure 3a. All distances in meters.

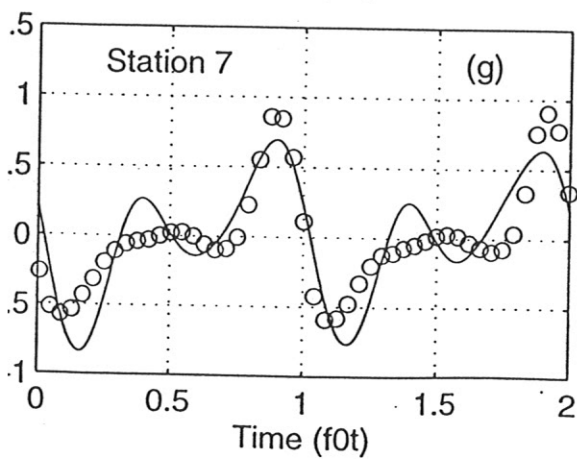
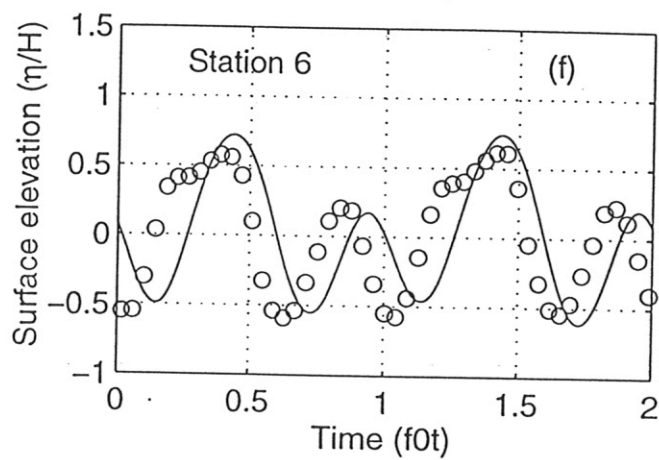
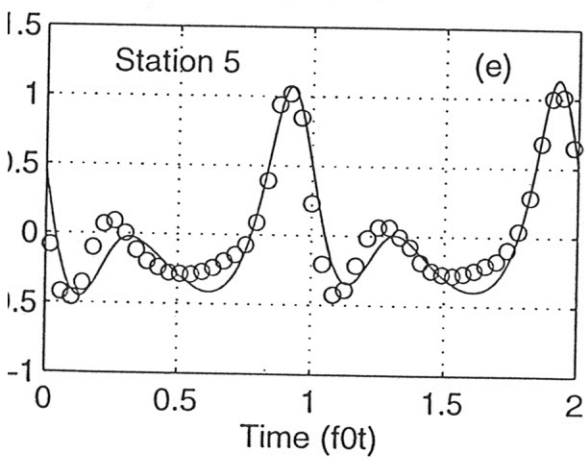
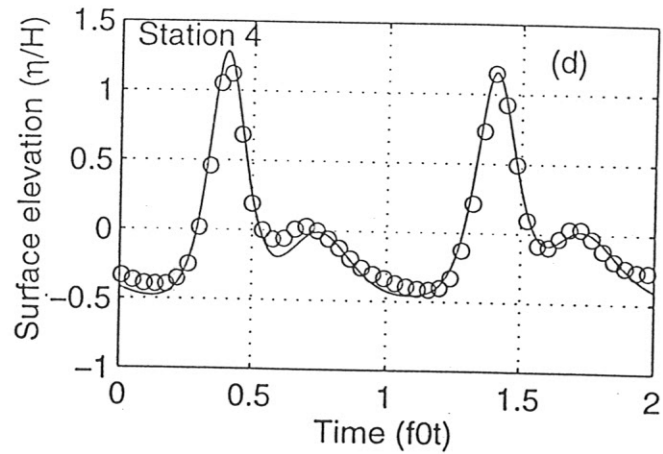
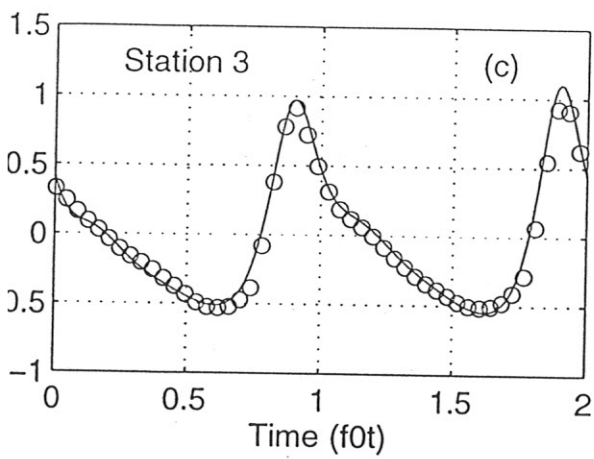
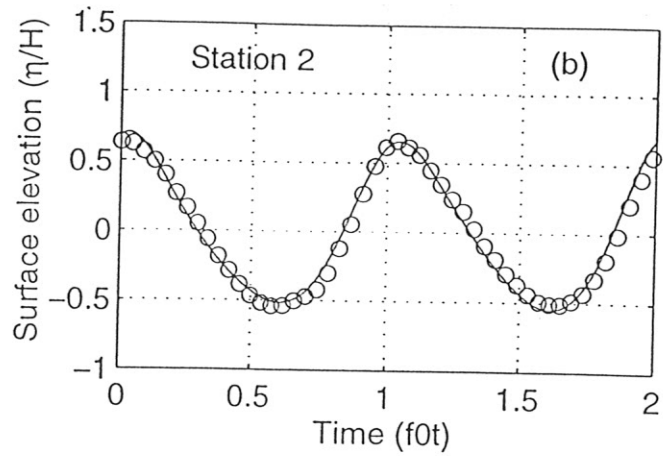
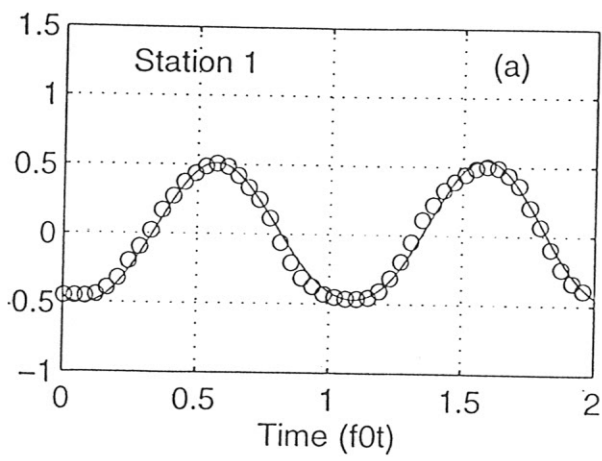


Figure 6 Comparison of the G-N II results with the experiments of Ohyama et al. (1994) at all gages for the long wave case. The free surface elevation,  $\eta/H$  as a function of time  $f_0t$ . The circles refer to the experimental data of Ohyama et al. (1994) and the solid line is the G-N II result.

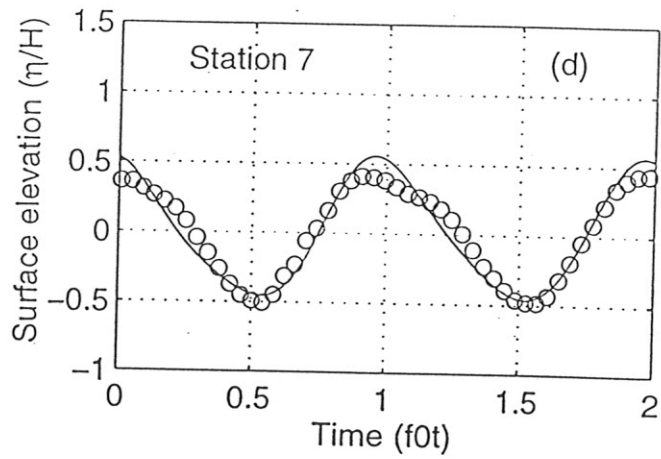
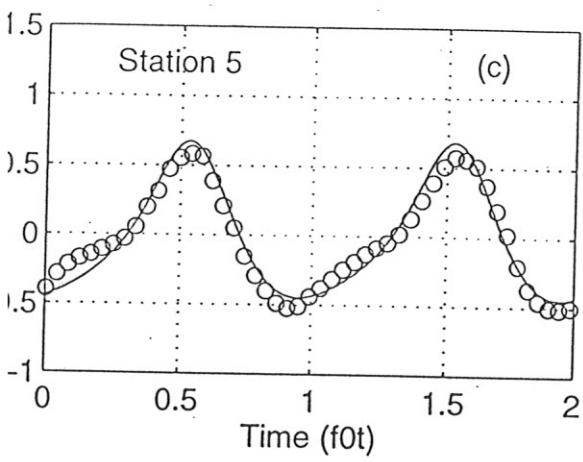
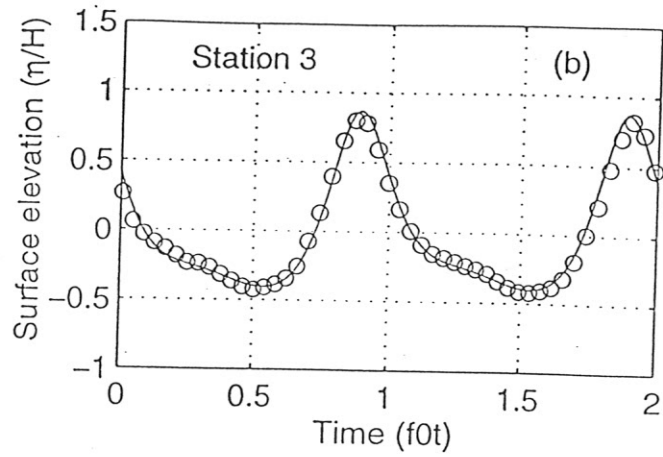
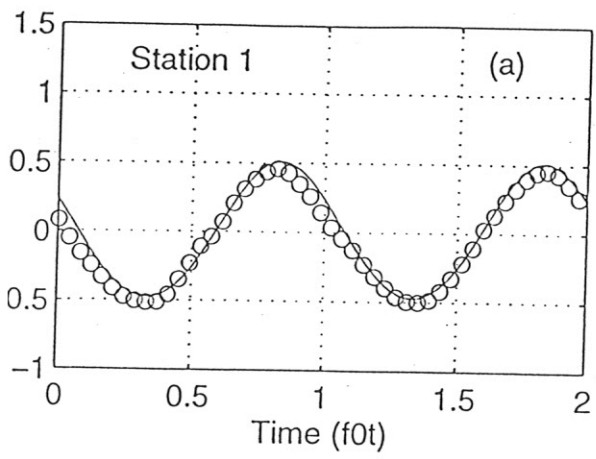


Figure 7 Comparison of the G-N II results with the experiments of Ohya et al. (1994) at different gages for the short wave case. The free surface elevation,  $\eta/H$  as a function of time  $f_0t$  at the following gages: (a) station 1, (b) station 3, (c) station 5 and (d) station 7. The circles refer to the experimental data of Ohya et al. (1994) and the solid line is the G-N II result.



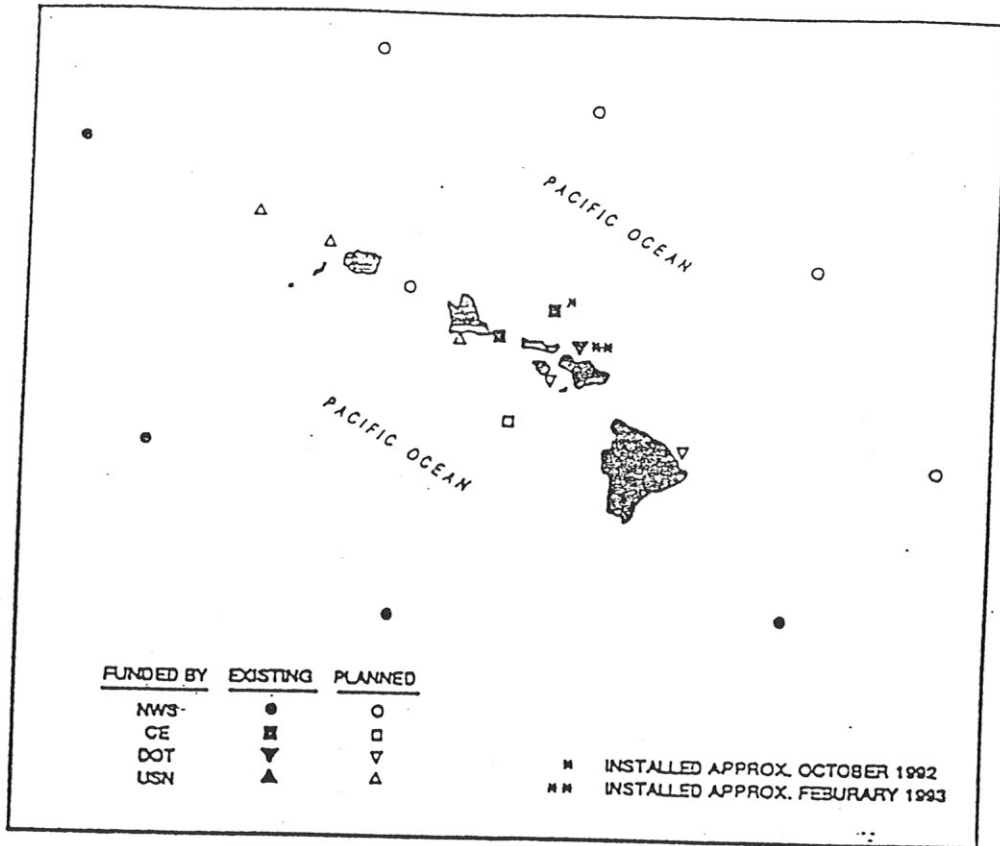


Figure 8 Locations of existing and proposed wave measurements in the Hawaiian region.

# All Islands Wave Patterns

(Moberly and Chamberlain, 1964)

Shoreline Certification Study: Fletcher and Hwang

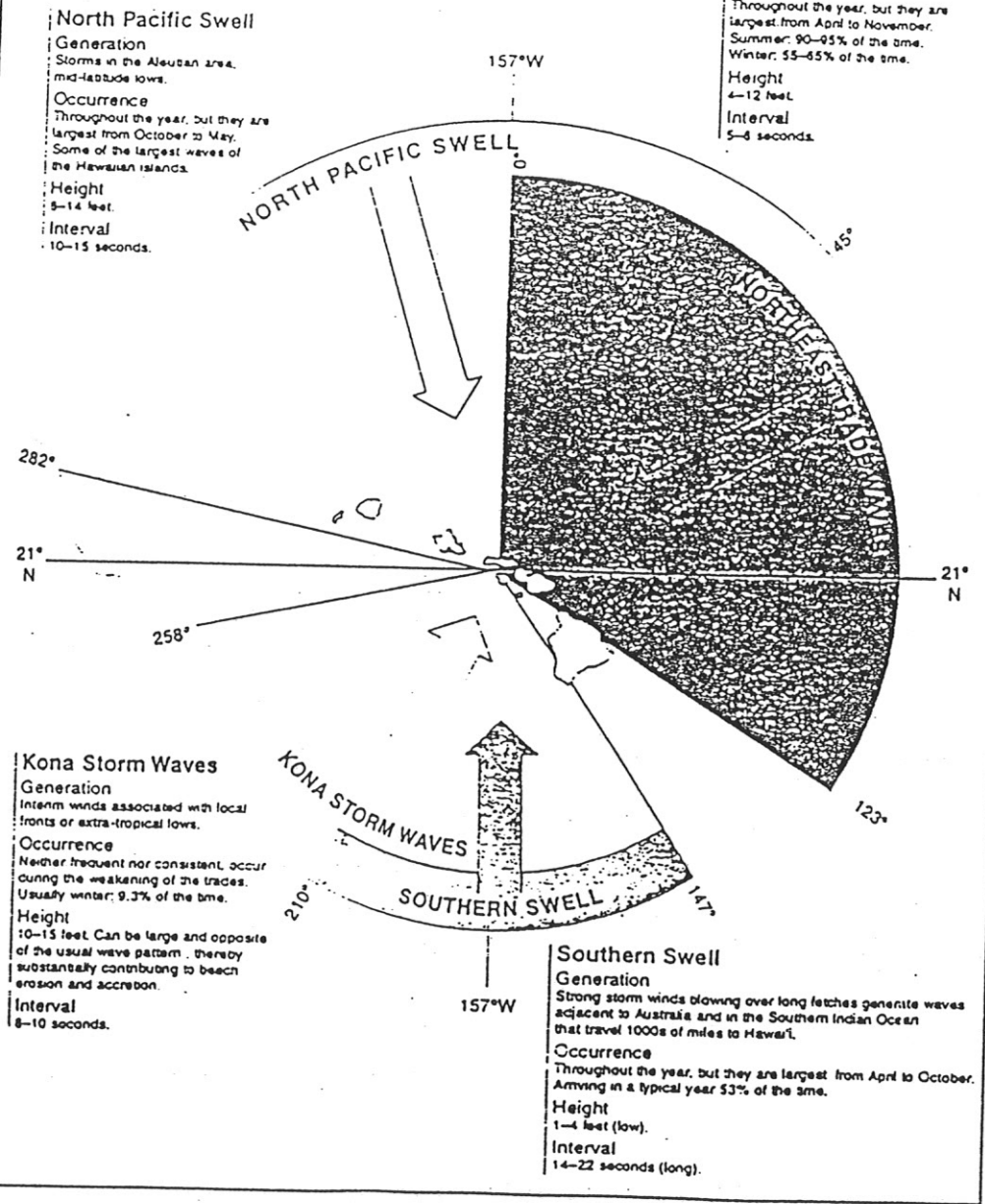


Figure 9 Primary sources of wave energy for the Hawaiian Islands, from Fletcher and Hwang, 1994.

Significant Wave Heights and Wave Periods for Hurricane Iniki  
(Makapu Waverider Buoy)

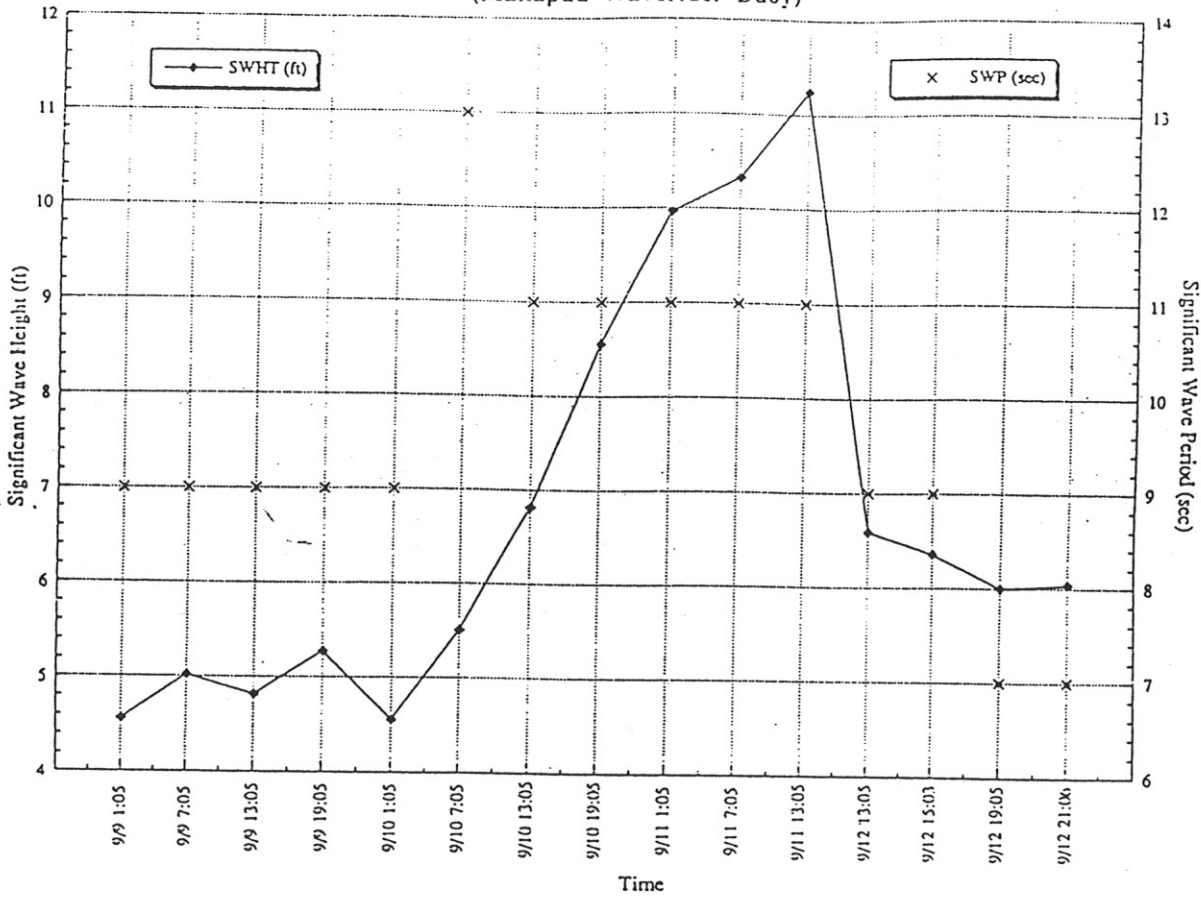


Figure 10 Significant wave height and period at Makapu'u Point during Hurricane Iniki, from Fletcher and Hwang, 1994.

Figure 11 Wave height (m) for a single wave component for Waikiki beach

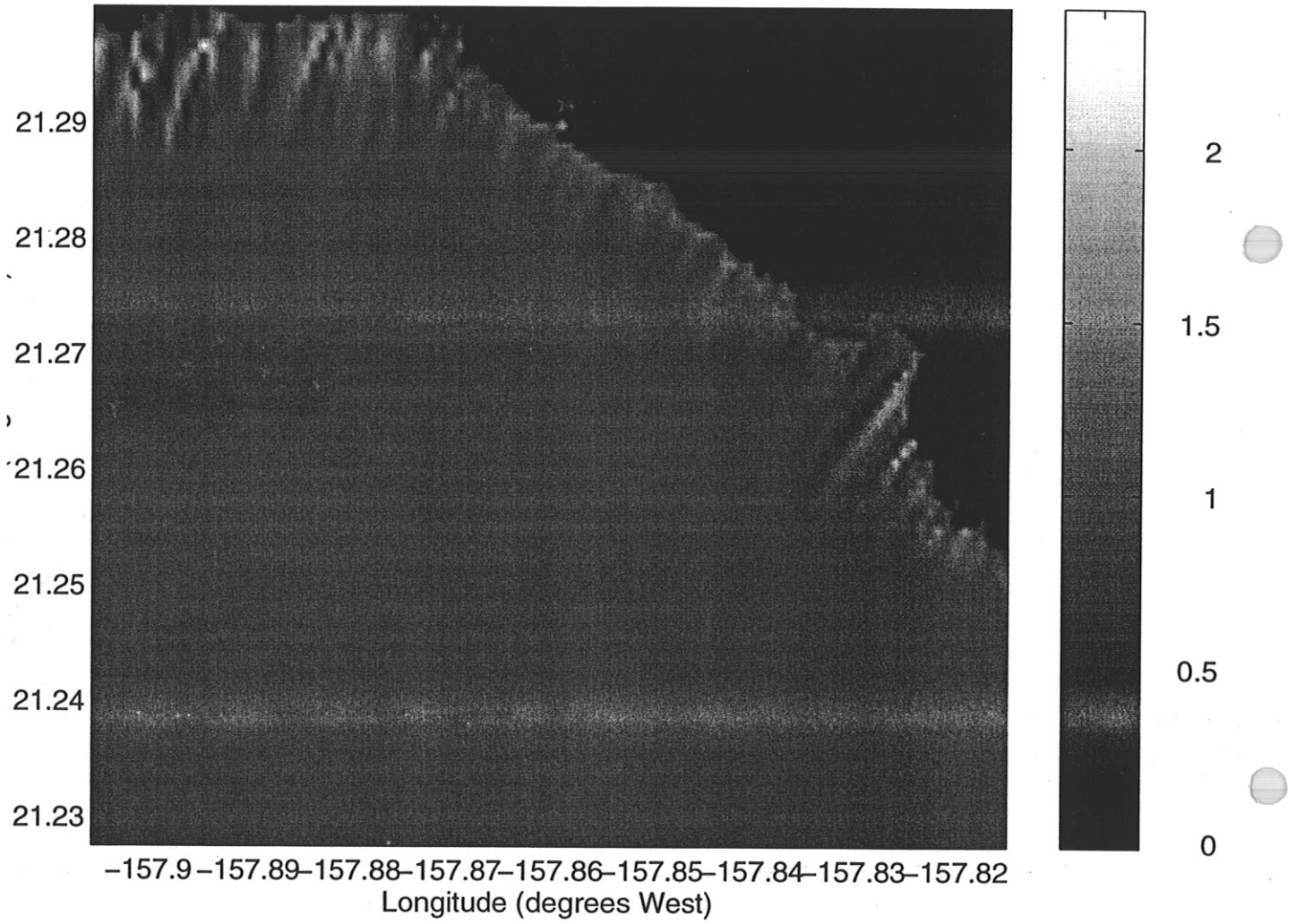
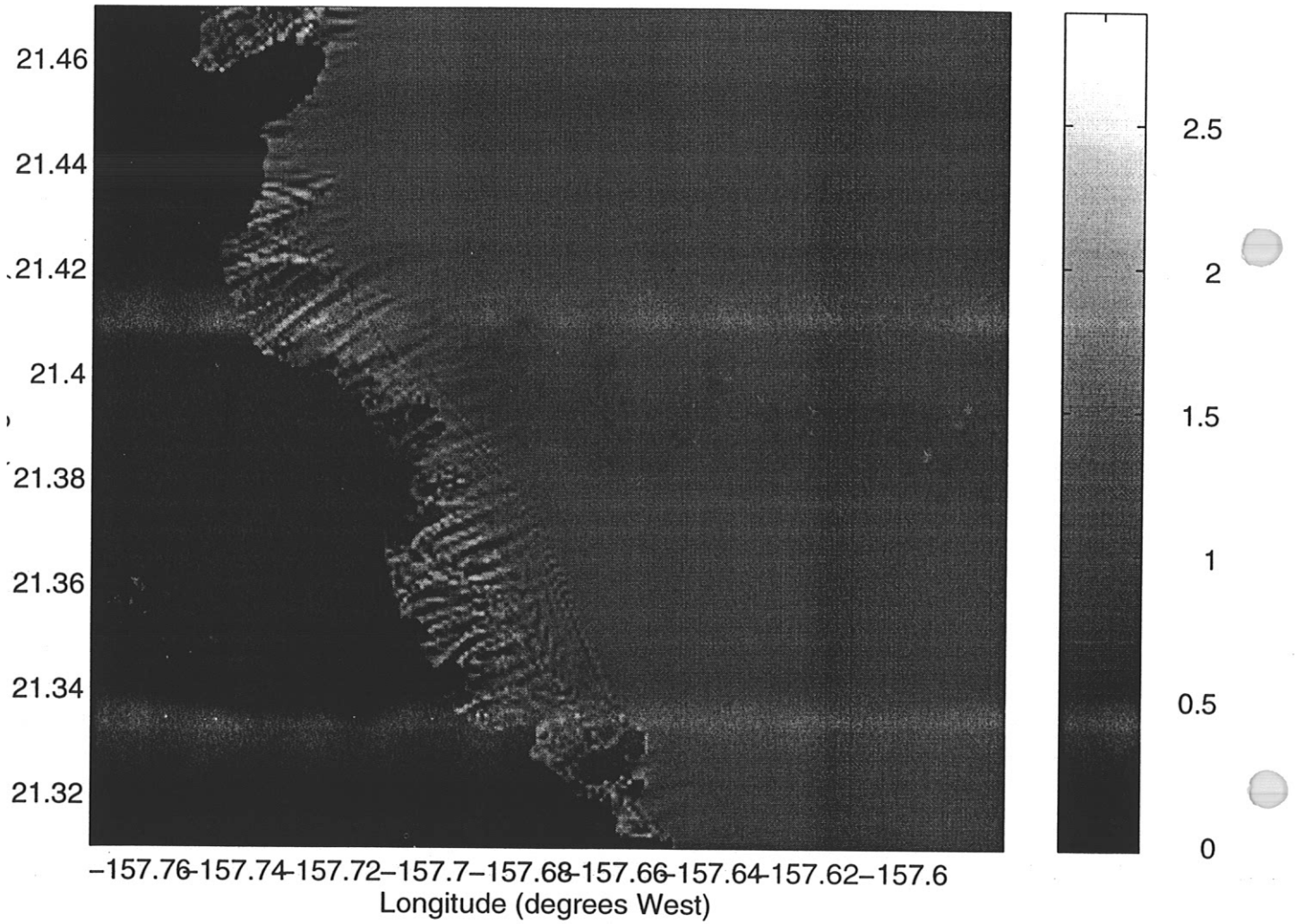


Figure 12 Wave height (m) for a single wave component for Kailua Bay



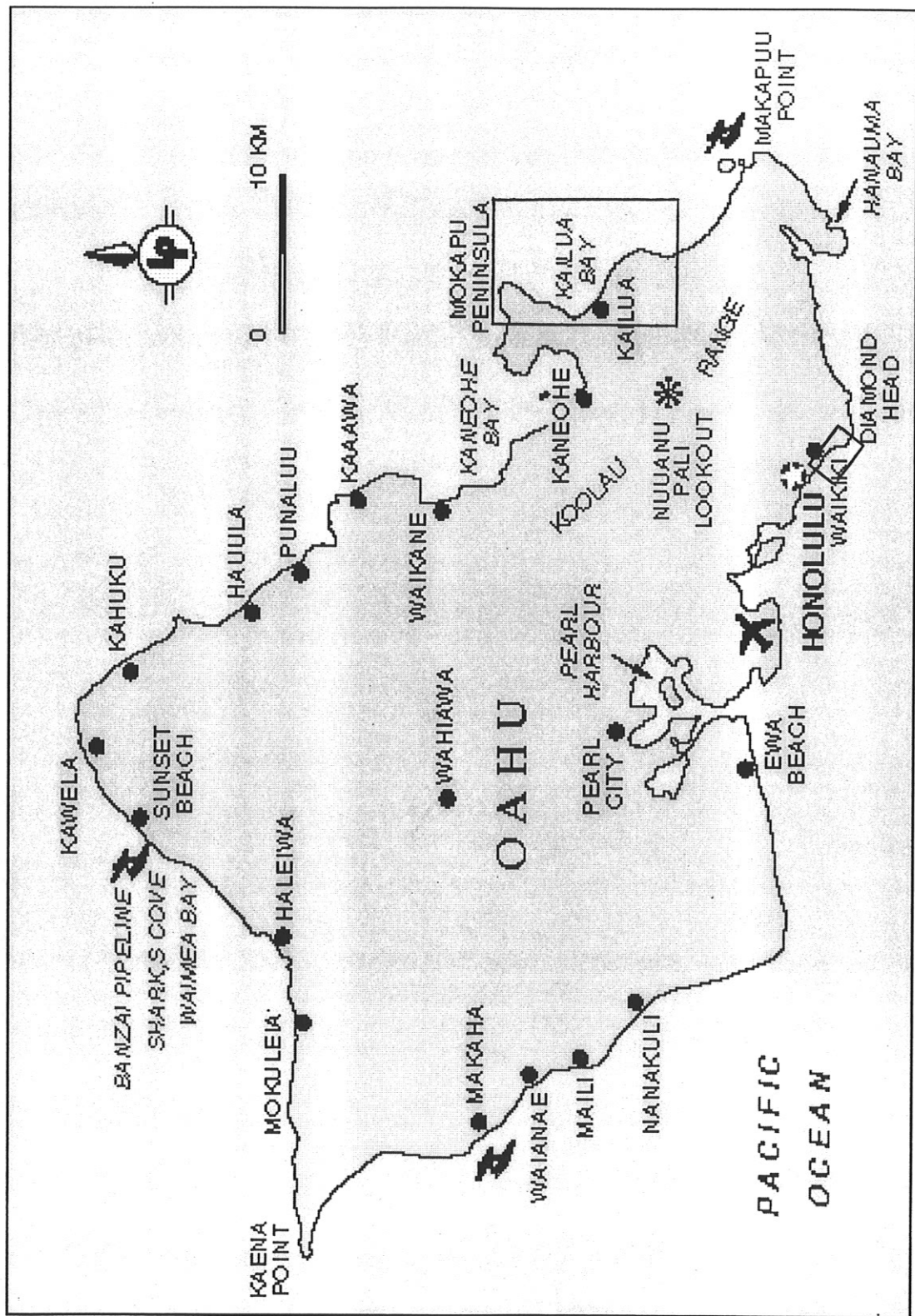


Figure 13 Two locations used for wave height simulation on the Island of Oahu.

Figure 14 Bathymetry (m) for Waikiki beach

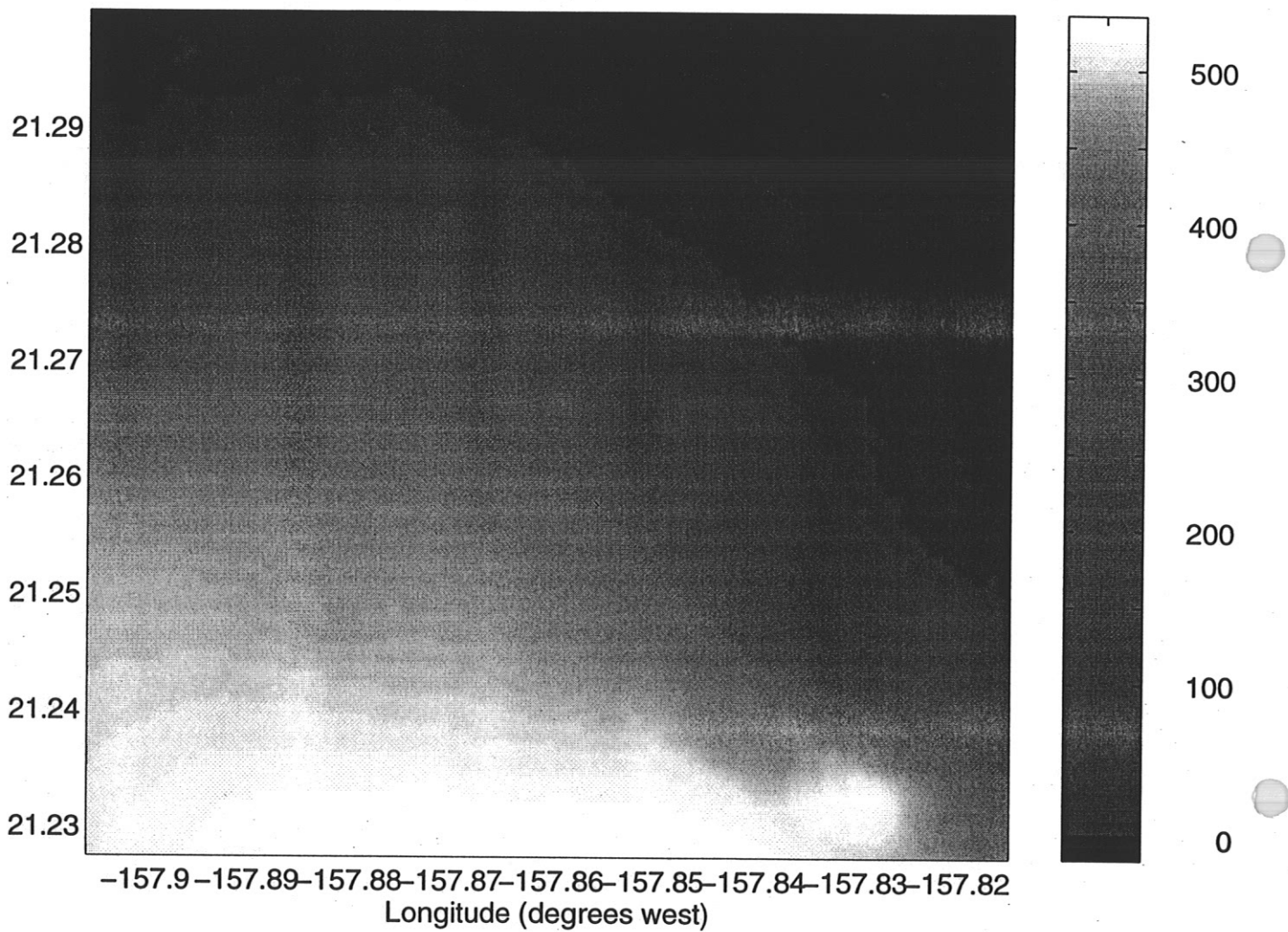


Figure 15 Bathymetry (m) for Kailua Bay

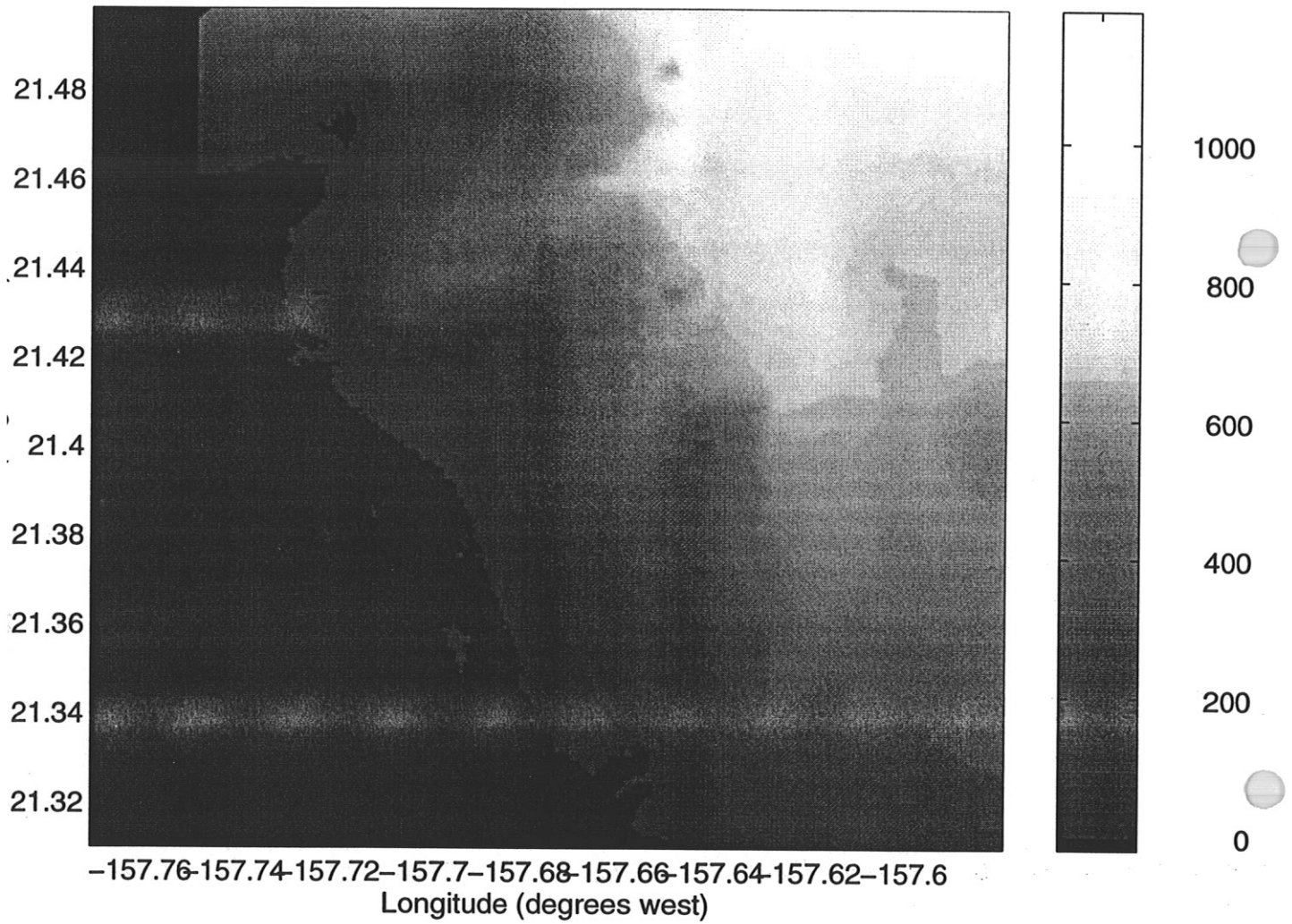




Figure 16 Wave height (m) for Waikiki beach

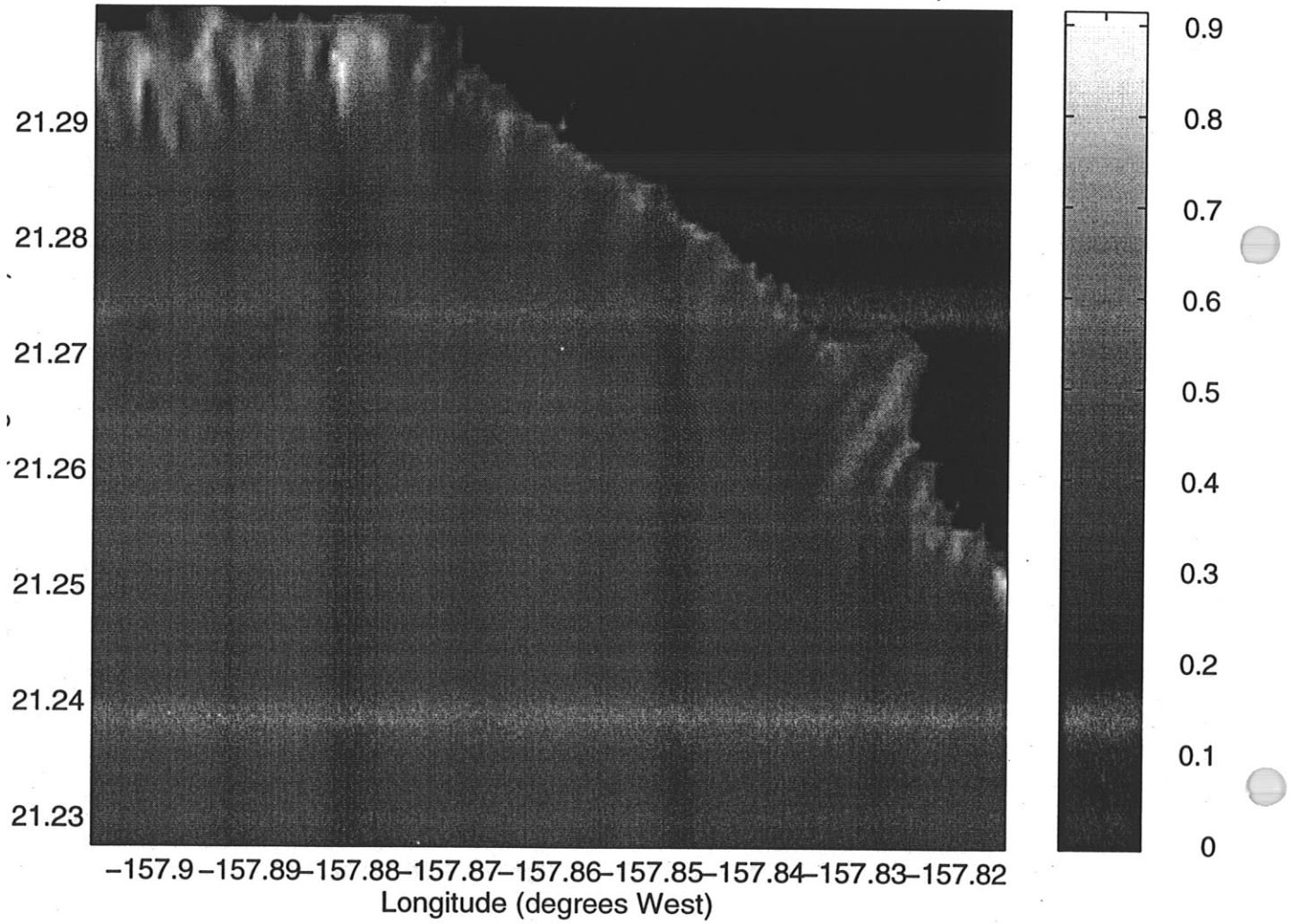


Figure 17 Wave height (m) for Kailua Bay

